Nonlinear susceptibilities of molecular aggregates: Enhancement of $\chi^{(3)}$ by size

Francis C. Spano and Shaul Mukamel
Department of Chemistry, University of Rochester, Rochester, New York 14627
(Received 24 July 1989)

We investigate the third-order nonlinear-optical susceptibility $\chi^{(3)}$ in molecular aggregates and its scaling with aggregate size. The aggregate is modeled as a collection of N-interacting, homogeneously broadened two-level systems, where the interaction includes both the static dipole-dipole coupling and superradiant coupling. Our expression for $\chi^{(3)}$, derived using Liouville-space Green-function techniques, contains contributions from excitons as well as biexcitons. The scaling of $\chi^{(3)}$ with aggregate size and its dependence on the laser detuning and homogeneous and inhomogeneous dephasing rates are analyzed. $\chi^{(3)}$ contains terms that scale as $\sim N^2$ and $\sim N(N-1)$. However, under off-resonant conditions these terms interfere destructively, resulting in a linear $\sim N$ scaling, which is precisely what is expected for N monomers. Detailed calculations of phase-conjugate degenerate four-wave mixing and pump-probe spectroscopy are performed. In the first case we predict the existence of a narrow dephasing-induced resonance superposed on the broader superradiant exciton line shape. Pump-probe spectroscopy shows a series of biexciton absorption lines, some of which are superradiantly broadened.

I. INTRODUCTION

Currently there is great interest in molecular aggregates or clusters, the optical properties of which have been studied in solution,[1] on metal and semiconductor surfaces,[2] and in molecular beams.[3] Of particular interest are J aggregates,[1,4–9] which form when certain dye molecules such as pseudo-isocyanine (PIC) are cooled in solution at a sufficiently high concentration. Upon aggregation the absorption spectrum of these systems dramatically narrows and shifts to the red. This has been attributed to motional narrowing of the inhomogeneous broadening in the excitonlike state, as proposed by Knapp.[5] J aggregates also display interesting excited-state dynamics;[6–9] in particular, an enhanced radiative decay rate that depends on aggregate size, as measured by various nonlinear-optical techniques.[6–8] The enhanced radiative rate may be attributed to the $\sim N^{1/2}$ scaling of the transition dipole moment, which results in a linear $\sim N$ scaling of the radiative decay rate with aggregate size N. The effect of homogeneous dephasing on the enhanced radiative rate was studied by Grad, Hernandez, and Mukamel[10] using an effective-Hamiltonian approach. It was shown that the pure dephasing $\hat{\Gamma}$ directly competes with the radiative damping $N\gamma$ (where γ is the monomer radiative rate). For large values of $\hat{\Gamma}/N\gamma$ the enhanced radiative rate $N\gamma$ is quenched and is reduced to the monomer value γ. In a previous publication[11] we have theoretically investigated the excited-state dynamics of J aggregates with intermolecular dipole-dipole coupling V and varying degrees of inhomogeneous broadening, and have established that the enhanced fluorescence rate is a result of microscopic superradiance.[12] A superradiant decay is observed as long as $N^3(\sigma/V)^2\pi^{-4} \ll 1$ and $\hat{\Gamma}/N\gamma \ll 1$. When either of these conditions is violated, the cooperativity is determined by a *coherence length* which is smaller than the aggregate size. As the homogeneous or inhomogeneous broadening is increased the coherence length decreases until the superradiant decay is destroyed, yielding the single-molecule result. It is interesting to note that when $V \gg \hat{\Gamma} \gg N\gamma$ the superradiance is destroyed but the transition frequency is still equal to the exciton frequency. This shows that different cooperative phenomena have different coherence lengths.

In the present paper we extend our investigation of molecular aggregates to include the third-order nonlinear susceptibility $\chi^{(3)}$.[13,14] Our main goal is to calculate the effect of aggregate size on $\chi^{(3)}$ and determine if large aggregates possess enhanced or giant nonlinear susceptibilities. Materials with large and fast nonlinear susceptibilities for off-resonant optical frequencies which are not absorbed by the medium are needed for optical switching applications in communications and optical computing. The ability to fabricate materials with desirable nonlinear properties is now an important engineering challenge. One complication is that materials with fast switching times will typically have smaller nonlinear susceptibilities, and the response speed is inversely proportional to the magnitude of the susceptibility. It has now been established that quantum-well structures,[13,15,16] conjugated organic molecules,[14,17,18] and unconjugated polysilanes[19] show enhanced third-order susceptibilities which depend on the confinement dimension in the first example, and chain length in the last two examples. Theoretical treatments of Wannier excitons in semiconductor microstructures (quantum dots, quantum wells)[20–24] predict an extremely large $\chi^{(3)}$ enhancement with size;[24] however, we are unaware of experiments which show giant enhancements of nonlinear susceptibilities. The present paper deals with the analogous problem for Frenkel excitons. Our starting point, as in Ref. 11, is the superradiant master equation.[12] We consider one-dimensional cy-

clic aggregates composed of N-coupled two-level systems and assume the linear dimension to be much smaller than an optical wavelength. We allow for both homogeneous broadening and inhomogeneous broadening within the motional narrowing regime. Homogeneous dephasing is described by the well-known Haken-Strobl model.[25] A completely quantum-mechanical expression for $\chi^{(3)}$ is derived which includes the effects of biexcitons; we do not invoke the semiclassical approximation. From the final expression for $\chi^{(3)}$, it is apparent that the size dependence arises from essentially two factors: the enhanced exciton and exciton-biexciton transition dipole moments which scale as $N^{1/2}$ and the superradiant decay rate which scales as N. For large N, the enhanced transition dipole moments combine to give an overall N^2 dependence to $\chi^{(3)}$. In contrast, the enhanced radiative rates which appear in the denominators act to reduce $\chi^{(3)}$. Since the pure dephasing competes directly with the size-dependent superradiant damping[12] it also has a profound effect on the size dependence of $\chi^{(3)}$. Laser detuning also plays an important role. When all applied E fields in a four-wave mixing experiment are far off resonance, and there are no resonant denominators in $\chi^{(3)}$ our expression reduces to the monomer result ($\chi^{(3)} \propto N$). This prediction, which contradicts previous arguments,[24] is a result of an interesting interference between terms in $\chi^{(3)}$ with N^2 and $N(N-1)$ prefactors (which arise from the enhanced oscillator strength). The complete N dependence which results from the combination of enhanced transition moments, superradiant damping rates, homogeneous dephasing rate, and laser detuning is quite complicated and must be separately analyzed for each particular nonlinear experiment. As an illustration, we evaluate the scaling properties of phase-conjugate degenerate four-wave mixing[26] (DFWM) when the pump is tuned to the exciton frequency, and show that the integrated $|\chi^{(3)}|^2$ spectrum ranges from an $\sim N^{-1}$ dependence to an $\sim N^4$ dependence as the homogeneous dephasing rate is increased from zero to a value much larger than the superradiant damping rate. In analyzing the DFWM spectrum we predict the existence of a narrow resonance which results from a dephasing-induced population transfer from the $k=0$ superradiant exciton state to the $N-1$ subradiant exciton states. This resonance provides an indirect measurement of subradiance, which is experimentally much harder to observe than superradiance because the small transition dipole of the subradiant state does not allow direct optical pumping.[27] Such narrow resonances have recently been observed in quantum wells[28] and are related to the dephasing-induced spectral holes in homogeneously broadened lines.[29] We also analyze the probe absorption spectrum in the presence of a pump beam for a system of aggregates. Unlike DFWM this technique directly probes the biexciton states which have been studied in great detail in CuCl.[30–33] Most theoretical treatments of biexcitons assume a simplified three-level system[33] or a two-boson model.[32] In our Frenkel exciton model we are able to exactly calculate the biexciton states for the nearest-neighbor coupling model. We show that, for odd N, there are in general $(N-1)/2$ biexcitons (labeled with $q=1,3,\ldots,N-1$) which can be directly excited via two-photon absorption from the aggregate ground state.

This paper is divided into eight sections. In the second section we present the model and the superradiant density-matrix equation of motion in terms of the collective exciton operators. In Sec. III we calculate the Liouville-space eigenvectors which are the exciton and biexciton coherences and populations. In Sec. IV we use Liouville-space Green functions[34] and the response-function formalism[35] to derive an expression for $\chi^{(3)}$ in the limit $\hat{\Gamma}=0$. In Sec. V pure dephasing is included perturbatively resulting in a more general expression for $\chi^{(3)}$. In Sec. VI we study the aggregate size dependence of $|\chi^{(3)}|^2$ and the narrow dephasing-induced resonances in phase-conjugate DFWM. Pump-probe absorption spectroscopy is dealt with in Sec. VII, and in the final section we summarize our findings.

II. EQUATION OF MOTION

In this article we consider cyclic, one-dimensional aggregates (N equally spaced molecules on a circle) with N odd. Each molecule is modeled as a two-level system with transition frequency ω_0. The calculation of $\chi^{(3)}$ is greatly simplified in this configuration. We believe, however, that our analysis and general conclusions regarding the cooperativity are not restricted to this special case.

The equation of motion which describes the electromagnetic interactions between the N molecular polarizations within the aggregate and between the aggregate polarization and the applied electromagnetic field is the superradiant master equation:[12]

$$\begin{aligned}\frac{d\rho}{dt} &= \sum_{n=1}^{N} i\omega_0[\rho, b_n^\dagger b_n] + \sum_{m\neq n}^{N} i\Omega_{mn}[\rho, b_m^\dagger b_n] \\ &\quad + \sum_{m,n=1}^{N} \gamma_{mn}[b_m \rho b_n^\dagger - \tfrac{1}{2}(b_m^\dagger b_n \rho + \rho b_m^\dagger b_n)] \\ &\quad + \frac{i\mu}{2\hbar}\sum_{n=1}^{N} E(\mathbf{r}_n,t)[\rho(t), b_n^\dagger + b_n] \,, \end{aligned} \tag{2.1}$$

where ρ is the density matrix of the aggregate and $b_n^\dagger$ and b_n are the Pauli creation and annihilation operators, respectively, for an excitation at site n, obeying the anticommutation relation:

$$[\hat{b}_m^\dagger, \hat{b}_n]_+ \equiv \hat{b}_m^\dagger \hat{b}_n + \hat{b}_n \hat{b}_m^\dagger = \delta_{mn} + 2\hat{b}_m^\dagger \hat{b}_n(1-\delta_{mn}) \,. \tag{2.2}$$

In Eq. (2.1), $E(r,t)$ is the applied electric field, μ is the transition dipole moment, and the coupling coefficients are given by[12]

$$\Omega_{mn} = \frac{3\gamma}{4}\left[(\cos^2\theta_{mn}-1)\frac{\cos(x)}{x} + (1-3\cos^2\theta_{mn})\left[\frac{\sin(x)}{(x)^2}+\frac{\cos(x)}{(x)^3}\right]\right] , \tag{2.3a}$$

$$\gamma_{mn}=\frac{3\gamma}{2}\left[(\cos^2\theta_{mn}-1)\frac{\sin(x)}{x}+(1-3\cos^2\theta_{mn})\left[\frac{\cos(x)}{(x)^2}-\frac{\sin(x)}{(x)^3}\right]\right], \tag{2.3b}$$

where $x=k_0 r_{mn}$ and $\theta_{mn}=\hat{\mathbf{p}}\cdot\hat{\mathbf{r}}_{mn}$. $\hat{\mathbf{p}}$ is a unit vector in the direction of the dipole moments, assumed parallel within an aggregate and $\hat{\mathbf{r}}_{mn}=(\mathbf{r}_m-\mathbf{r}_n)/r_{mn}$ is the unit position vector between site m and n. We also have $k_0=\omega_0/c$.

Using the translational symmetry of our model we define collective creation and annihilation operators according to

$$b_k^\dagger=N^{-1/2}\sum_{n=1}^{N}\exp\left[\frac{i2\pi k(n-1)}{N}\right]b_n^\dagger , \tag{2.4}$$

with $b_k=(b_k^\dagger)^\dagger$. The reverse transformation is

$$b_n^\dagger=N^{-1/2}\sum_{k=0}^{N-1}\exp\left[\frac{-i2\pi k(n-1)}{N}\right]b_k^\dagger . \tag{2.5}$$

The collective operators b_k and $b_k^\dagger$ obey the following commutation relationship:

$$[b_k,b_{k'}^\dagger]=\delta_{kk'}-\frac{2}{N}\sum_{n=1}^{N}b_n^\dagger b_n . \tag{2.6}$$

Because of the second term on the right-hand side, b_k and $b_k^\dagger$ are not boson operators. They can only be treated as bosons for infinite crystals when $N\to\infty$ and in linear optics when $\langle b_n^\dagger b_n\rangle$ is very small. However, for nonlinear optics of small aggregates we cannot invoke the boson approximation.

Equation (2.1) can now be partitioned as

$$\frac{d}{dt}\rho(t)=-i(L_1+L_2+L_{\rm int})\rho(t) , \tag{2.7}$$

where L_1, L_2, and $L_{\rm int}$ are Liouville operators, defined by their action on an arbitrary operator Q as

$$L_1Q=-\sum_{k=0}^{N-1}\omega(k)[Q,b_k^\dagger b_k]-\sum_{k=0}^{N-1}\frac{i}{2}\gamma(k)(b_k^\dagger b_k Q+Qb_k^\dagger b_k) , \tag{2.8a}$$

$$L_2Q=i\sum_{k=0}^{N-1}\gamma(k)b_k Qb_k^\dagger , \tag{2.8b}$$

$$L_{\rm int}=\frac{-\mu E(\mathbf{r},t)}{2\hbar}[\hat{b}_0+\hat{b}_0^\dagger,Q] . \tag{2.8c}$$

The zero subscript in b_0 refers to $k=0$ and the functions $\omega(k)$ and $\gamma(k)$ are defined by

$$\omega(k)=\omega_0+\sum_{n=1}^{N}\Omega_{1n}\exp\left[\frac{i2\pi k(n-1)}{N}\right] , \tag{2.9a}$$

$$\gamma(k)=\sum_{n=1}^{N}\gamma_{1n}\exp\left[\frac{i2\pi k(n-1)}{N}\right] , \tag{2.9b}$$

where, because of the translation symmetry, the sums may be evaluated about any of the N molecules [molecule "1" in Eq. (2.9)].

In this article we assume that the aggregate is small compared to an optical wavelength $k_0 r_{mn}\ll 1$, so that all $E(\mathbf{r}_n,t)$ can be replaced by $E(\mathbf{r},t)$ in $L_{\rm int}$. In this limit we further have

$$\Omega_{mn}=\frac{3\gamma}{4}\frac{(1-3\cos^2\theta_{mn})}{(k_0 r_{mn})^3}\equiv V_{mn} , \tag{2.10a}$$

and

$$\gamma_{mn}=\gamma . \tag{2.10b}$$

where V_{mn} is the static dipole-dipole coupling and γ is the single-molecule spontaneous emission rate. For simplicity we shall include only the nearest-neighbor coupling in the real part of the interaction V_{mn}. (This approximation, although not necessary at this point, simplifies the calculation of the biexciton states, so we invoke it hereafter.) From Eqs. (2.9) and (2.10) it follows that

$$\omega(k)=\omega_0+2V\cos\left[\frac{2\pi(k-1)}{N}\right] , \tag{2.11a}$$

$$\gamma(k)=(N\gamma/2)\delta_{k,0} . \tag{2.11b}$$

The equation of motion (2.7) and Eq. (2.8) with the coupling in Eq. (2.11) define the basic model system which will be studied in this article. In this model we do not include explicitly the coupling to other (bath) degrees of freedom. This will be done in Sec. V where we introduce homogeneous broadening. Inhomogeneous broadening may be incorporated by assuming that the transition frequency for the absorber at site m is $\omega_0+\delta\omega_m$. In this case we lose the translational symmetry. Nevertheless, if the inhomogeneous absorption linewidth is not too large, it can be incorporated perturbatively. This is done in Sec. VI.

III. EXCITON AND BIEXCITON OPERATORS

The ground-state density matrix of the aggregate is denoted as $|0\rangle\langle 0|$ and represents a state with all molecules in the ground electronic level. A complete basis set of operators which can be used to represent an arbitrary density matrix may be generated by acting with any combination of $b_k^\dagger(b_k)$ operators on the bra (right) or the ket (left) of the vacuum state. The calculation of $\chi^{(3)}$ requires only a limited number of operators consisting of the result of one or two operations of b_k and $b_k^\dagger$ on the ground-state density matrix. These will be defined below.

We first define exciton coherence operators generated when the collective creation operator $b_k^\dagger(b_k)$ acts once to the left (right) of the vacuum state:

$$|b(k)\rangle\rangle\equiv b_k^\dagger|0\rangle\langle 0| ,$$

$$|\bar{b}(k)\rangle\rangle\equiv|0\rangle\langle 0|b_k ,$$

where $|\ldots\rangle\rangle$ denotes the corresponding Liouville-space ket.[34] The bar above the $b(k)$ indicates an exciton with

wave vector k on the right side (bra). Operating with L_1 from Eq. (2.8a) it is evident that $|b(k)\rangle\rangle$ is a Liouville-space eigenvector of L_1:

$$L_1|b(k)\rangle\rangle=[-\omega(k)-i\gamma(k)]|b(k)\rangle\rangle \ . \tag{3.1}$$

Similarly, an exciton population ($k=k'$) or exciton-exciton coherence ($k\neq k'$) is created by application of $b_k^\dagger$ to the right and $b_{k'}$ to the left of the ground-state density matrix $|0\rangle\langle 0|$:

$$|b(k)\bar{b}(k')\rangle\rangle\equiv b_k^\dagger|0\rangle\langle 0|b_{k'} \ .$$

The operator $|b(k)\bar{b}(k')\rangle\rangle$ is also a Liouville-space eigenvector of L_1:

$$L_1|b(k)\bar{b}(k')\rangle\rangle=\{\omega(k')-\omega(k) -i[\gamma(k)+\gamma(k')]\}|b(k)\bar{b}(k')\rangle\rangle \ . \tag{3.2}$$

From Eqs. (3.1), (3.2), and (2.11b) we see that the $k=0$ exciton population as well as the exciton coherence decays N times faster than the corresponding quantities for an independent single molecule. The superradiant nature of the $k=0$ exciton state is discussed in detail in Ref. 11. Also notice that the $k\neq 0$ exciton does not radiate at all. This "subradiance" results from the absence of a transition dipole moment between the ground state and the $k\neq 0$ exciton state.

The biexciton coherence subspace is spanned by operators which result from the application of two collective creation (annihilation) operators to the left (right) of the vacuum state:

$$|b(k)b(k')\rangle\rangle\equiv b_k^\dagger b_{k'}^\dagger|0\rangle\langle 0| \ ,$$

$$|\bar{b}(k)\bar{b}(k')\rangle\rangle\equiv|0\rangle\langle 0|b_k b_{k'} \ .$$

The biexciton operators which are eigenvectors of L_1 are more difficult to derive. They are not simply the result of two interactions with $b_k^\dagger$ to the right of the ground-state density matrix yielding $|b(k)b(k)\rangle\rangle$ since $b_k^\dagger$ and b_k are not boson operators. This can easily be checked by application of L_1:

$$L_1|b(k')b(k'')\rangle\rangle=-\{\omega(k')+\omega(k'')+i[\gamma(k')+\gamma(k'')]\}|b(k')b(k'')\rangle\rangle + \frac{2}{N}\sum_{k=k'}^{N-1-k'}[\omega(k+k')+i\gamma(k+k')]|b(k'+k)b(k''-k)\rangle\rangle \ . \tag{3.3}$$

In order to calculate the biexciton eigenbasis we first define the following translationally invariant operators:

$$|C(k,s)\rangle\rangle=\frac{1}{\sqrt{N}}\sum_r \exp\left[\frac{i2\pi kr}{N}\right]b_{r-s/2}^\dagger b_{r+s/2}^\dagger|0\rangle\rangle \ , \tag{3.4}$$

where $|0\rangle\rangle$ is the Liouville-space notation for the ground-state density matrix $|0\rangle\langle 0|$. The index r is equal to $(m+n)/2$, where the sites m and n are separated by a distance s. The index s can take on values from 1 to $N-1$; $s=0$ and $s=N$ are not allowed since two excitations cannot reside on the same molecule. The operators defined in Eq. (3.4) are overcomplete and therefore not orthogonal since $|C(k,s)\rangle\rangle=|C(k,N-s)\rangle\rangle$. We can use these operators to construct the biexciton eigenbasis of L_1 when $N\geq 5$:

$$|B(k,q)\rangle\rangle=\frac{2}{\sqrt{N}}\sum_{s=1}^{(N-1)/2}\sin\left[\frac{\pi qs}{N}\right]|C(k,s)\rangle\rangle \ , \tag{3.5}$$

where the sum is now over only $(N-1)/2$ states. [For $N=3$ the biexciton eigenbasis is given by $|B(k,1)\rangle\rangle=|C(k,1)\rangle\rangle$.] There are $(N-1)/2$ orthogonal operators (N is odd) for each value of k; since there are N values of k there is a total of $N(N-1)/2$ biexciton states which is the expected number based on the total number of independent $b_m^\dagger b_n^\dagger|0\rangle$ states. Operation of L_1 on the biexciton states yields

$$L_1|B(k,q)\rangle\rangle=[-\Omega(k,q)-i\Gamma(k,q)]|B(k,q)\rangle\rangle - i\sum_{q'\neq q}\Gamma'(k,q,q')|B(k,q')\rangle\rangle \ , \tag{3.6}$$

where the biexciton frequencies and damping rates are given by

$$\Omega(k,q)=2\omega_0+4V\cos\left[\frac{\pi k}{N}\right]\cos\left[\frac{\pi q}{N}\right] \ , \tag{3.7a}$$

$$\Gamma(k,q)=\begin{cases}\dfrac{2\gamma}{N}\left\{\dfrac{1}{4}\left[\cot\left[\dfrac{(q+k)\pi}{2N}\right]+\cot\left[\dfrac{(q-k)\pi}{2N}\right]\right]^2\right\} & \text{for } k \text{ even} \ , \\ \left[\dfrac{N\gamma}{2}\right]\delta_{kq} & \text{for } k \text{ odd} \ ,\end{cases} \tag{3.7b}$$

and $q=1,3,\ldots,N-2$ in all cases. (For $N=3$ we have $\Omega(k,1)=2\omega_0+2V\cos(2\pi k/3)$ and $\Gamma(k,1)=\gamma[1+\cos(2\pi k/3)]$). Strictly speaking, the basis set $|B(k,q)\rangle\rangle$ does not diagonalize the imaginary part of L_1. There remain nonzero off-diagonal matrix elements :

$$\Gamma'(k,q,q')=\langle\langle B(k,q)|\mathrm{Im}[L_1]|B(k,q')\rangle\rangle \ .$$

Using standard perturbation theory, however, it is

straightforward to derive the conditions under which the corrections to the first-order eigenvalues and eigenvectors are negligibly small; the difference between the real parts of any diagonal elements, $\Omega(k,q)-\Omega(k,q')$, must be much greater than $\Gamma'(k,q,q')$. It is easy to show that $\Gamma'(k,q,q')<N\gamma$ and therefore we have, for the $k=0$ subspace, the condition

$$\left|\frac{\Gamma'(0,q,q')}{\Omega(0,q)-\Omega(0,q')}\right|<\frac{N^3\gamma}{16V\pi^2}\ll 1 . \tag{3.8}$$

When this condition holds, the off-diagonal part of the coupling, Γ', can be neglected and the operators $|B(k,q)\rangle\rangle$ provide a good approximate eigenbasis of L_1 whose eigenvalues are the biexciton frequencies and radiative decay rates given by Eq. (3.7). For a value of $V=10^9\gamma$ (two oscillating dipoles with $\omega_0=3\times10^{15}$ separated by 1 Å, with $\theta_{mn}=0$) Eq. (3.7) is valid for $N<5000$.

IV. CALCULATION OF $\chi^{(3)}$

In this section we derive a general expression for $\chi^{(3)}$ using the Liouville-space Green-function technique.[34] In order to clarify the presentation, we first consider the isolated aggregate without line broadening and delay the inclusion of homogeneous dephasing until Sec. V.

A four-wave mixing experiment may involve as many as three applied electric fields; the total applied field is given by the superposition

$$E(\mathbf{r},t)=\sum_{j=1}^{3}[E_j\exp(i\mathbf{k}_j\cdot\mathbf{r}-i\omega_j t)+E_j^*\exp(-i\mathbf{k}_j\cdot\mathbf{r}+i\omega_j t)] , \tag{4.1}$$

where ω_j, $\mathbf{k}_j$, and E_j are the frequency, wave vector, and electric field envelope of the jth field, respectively. In this paper we consider only the cw case so that all E_j are time independent. The third-order polarization for an aggregate at position $\mathbf{r}$ with $k_0 r_{mn}\ll 1$ can be written as

$$P(\mathbf{r},t)=\sum_{\mathbf{k}_s,\omega_s}\exp(i\mathbf{k}_s\cdot\mathbf{r}-\omega_s t)P(\mathbf{k}_s,t) , \tag{4.2}$$

where $\mathbf{k}_s=\pm\mathbf{k}_m\pm\mathbf{k}_n\pm\mathbf{k}_q$ and $\omega_s=\pm\omega_m\pm\omega_n\pm\omega_q$ with $m,n,q=1$, 2, or 3, and any combination of plus and minus signs are allowed. Hereafter we choose the particular combination $\omega_s=\omega_1+\omega_2+\omega_3$ and $\mathbf{k}_s=\mathbf{k}_1+\mathbf{k}_2+\mathbf{k}_3$. Any other combination can be represented by changing one or more $\mathbf{k}_j$ to $-\mathbf{k}_j$, ω_j to $-\omega_j$, and E_j to E_j^*. The polarization is related to the applied electric fields via the third-order susceptibility:

$$P(\mathbf{k}_s,t)=\chi^{(3)}(-\omega_s;\omega_1,\omega_2,\omega_3)E_1E_2E_3 . \tag{4.3}$$

The nonlinear susceptibility may be evaluated using third-order perturbation theory[34,35] and is given by

$$\chi^{(3)}(-\omega_s;\omega_1,\omega_2,\omega_3)=\sum_p R(\omega_1+\omega_2+\omega_3,\omega_1+\omega_2,\omega_1) . \tag{4.4}$$

The material response function

$$R(\omega_m+\omega_n+\omega_q,\omega_m+\omega_n,\omega_n)$$

is defined as

$$R(\omega_m+\omega_n+\omega_q,\omega_m+\omega_n,\omega_m)=\langle\langle V|\mathcal{G}^0(\omega_m+\omega_n+\omega_q)\mathcal{V}\mathcal{G}^0(\omega_m+\omega_n)\mathcal{V}\mathcal{G}^0(\omega_m)\mathcal{V}\rho(-\infty)\rangle\rangle , \tag{4.5}$$

where $\rho(-\infty)$ is the equilibrium density matrix. The aggregate polarization operator V is given by

$$V=\mu\sum_{n=1}^{N}(\hat{b}_n^\dagger+\hat{b}_n)=N^{1/2}\mu(\hat{b}_0^\dagger+\hat{b}_0) , \tag{4.6}$$

and the Liouville operator $\mathcal{V}$, which represents the interaction of the applied field with the aggregate dipole under the dipole approximation, is defined by

$$\mathcal{V}|Q\rangle\rangle\equiv|[V,Q]\rangle\rangle , \tag{4.7}$$

where $|Q\rangle\rangle$ is an arbitrary operator. The frequency-dependent Green function $\mathcal{G}^0(\omega)$ is[34]

$$\mathcal{G}^0(\omega)=\frac{1}{\omega-L_1-L_2} . \tag{4.8}$$

The three Green functions in Eq. (4.5) appear in chronological order from right to left. The system first interacts with the field E_m. The single-photon Green function $\mathcal{G}^0(\omega_m)$ describes the evolution of the system until the time of the second interaction which is with the field E_n. Subsequent propagation is described by the two-photon Green function $\mathcal{G}^0(\omega_m+\omega_n)$. Following the third interaction with field E_q, the evolution is represented by the three-photon Green function $\mathcal{G}^0(\omega_m+\omega_n+\omega_q)$. The response function R in Eq. (4.5) is found by multiplying the final state of the system by V and taking the trace. In the nonlinear susceptibility $\chi^{(3)}$, the fields E_1, E_2, and E_3 can interact in any order in time. The summation $\sum_p$ appearing in Eq. (4.4) is over all $3!=6$ permutations of the frequencies ω_1, ω_2, and ω_3 which account for all possible time orderings of the external field interactions.

The evaluation of the response function in Eq. (4.5) is tedious but straightforward. For a system of noninteracting two-level systems Eq. (4.5) yields eight terms (or Liouville-space pathways) for a given ordering of the three electric fields. These arise from the eight possible ways the three $\mathcal{V}$'s can operate, i.e., each operation yields two terms according to Eq. (4.7), one a result of the V acting to the right of the initial operator, and one from the V acting to the left. The eight pathways afford a simple graphical representation.[34] In our case the operation

of $\mathcal{V}$ on an intermediate coherence or population containing a single excited state in the bra or ket yields both a double excited state (biexciton) and the ground state, depending on whether b_0 or $b_0^\dagger$ operates in Eq. (4.7). For example, $\mathcal{V}|b(0)\rangle\rangle = N^{1/2}\mu\{[|b(0)b(0)\rangle\rangle + |0\rangle\rangle] - |\bar{b}(0)\rangle\rangle\}$. The first two terms are a result of action from the left and the last term comes from action on the right. When one takes into account biexciton states, the total number of terms becomes 16 (for each particular time ordering of the interactions). Of these, half involve only the exciton state and half involve both exciton and biexciton states. As an example of this classification we show, in Fig. 1, Feynman diagrams[36] corresponding to (a) an all-exciton term and (b) a mixed exciton-biexciton term contributing to $\chi^{(3)}(-\omega_s;-\omega_3,\omega_2,\omega_1)$.

The Green functions needed to evaluate the response function in Eq. (4.5) are simple to evaluate since we know the eigenfunctions of L_1. The inclusion of L_2 does not effect the diagonal elements of $\mathcal{G}^0$ in the exciton-biexciton basis set as is shown in Appendix A. From Eq. (4.8) we have

$$\langle\langle b(k)|\mathcal{G}^0(\omega)|b(k)\rangle\rangle = \frac{1}{\omega+\omega(k)+i\gamma(k)}\ , \tag{4.9a}$$

$$\langle\langle b(k)\bar{b}(k')|\mathcal{G}^0(\omega)|b(k)\bar{b}(k')\rangle\rangle = \frac{1}{\omega+[\omega(k)-\omega(k')]+i[\gamma(k)+\gamma(k')]}\ , \tag{4.9b}$$

$$\langle\langle B(k,q)|\mathcal{G}^0(\omega)|B(k,q)\rangle\rangle = \frac{1}{\omega+\Omega(k,q)+i\Gamma(k,q)}\ , \tag{4.9c}$$

$$\langle\langle B(k,q)\bar{b}(k')|\mathcal{G}^0(\omega)|B(k,q)\bar{b}(k')\rangle\rangle = \frac{1}{\omega+[\Omega(k,q)-\omega(k')]+i[\Gamma(k,q)+\gamma(k')]}\ . \tag{4.9d}$$

Equation (4.9d) is the propagator for the exciton-biexciton coherence operator $|B(k,q)\rangle\langle b(k')|$ represented by $|B(k,q)\bar{b}(k')\rangle\rangle$ in Liouville-space notation. It should be noted that expressions (4.9a) and (4.9b) are exact, whereas (4.9c) and (4.9d) were evaluated by neglecting Γ' in accordance with condition (3.8). In addition to the diagonal Green-function matrix elements, there is one special class of nondiagonal elements which are nonzero because of L_2. This Liouville operator can couple the state $|b_0 Q b_0^\dagger\rangle\rangle$ to the state $|Q\rangle\rangle$. For the aggregate $\chi^{(3)}$ there are only two relevant elements, $\langle\langle b(0)|\mathcal{G}^0(\omega)|B(0,q)\bar{b}(0)\rangle\rangle$ and $\langle\langle 0|\mathcal{G}^0(\omega)|b(0)\bar{b}(0)\rangle\rangle$. In Appendix B we evaluate these matrix elements and show that the first is negligible when $N\gamma \ll |\Omega(0,q)-2\omega(0)|$ and the second element, which is responsible for the increase in ground-state population due to superradiant decay in the exciton population, is given by

$$\langle\langle 0|\mathcal{G}^0(\omega)|b(0)\bar{b}(0)\rangle\rangle = \frac{1}{\omega} - \frac{1}{\omega+iN\gamma}\ . \tag{4.10}$$

This term allows an additional pathway in the evaluation of $\chi^{(3)}$. For example, after two interactions with the applied field to produce an exciton population, the system may either remain in the exciton population [with its evolution described by the Green function in Eq. (4.9b)] or may return to the ground state via superradiant decay. This additional pathway must also be included in evaluating $\chi^{(3)}$ and is responsible for preserving the condition $\mathrm{Tr}\rho(t)=1$ for all times.[29(b)]

We are now in a position to write down the full expression for the third-order susceptibility, $\chi^{(3)}$ This consists of evaluating all possible pathways in the response function and inserting the expressions for the exciton and biexciton propagators [Eq. (4.9)]. When this is done we get

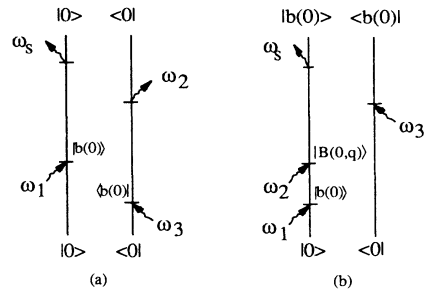

FIG. 1. Feynman diagrams corresponding to two terms in the expression for $\chi^{(3)}(-\omega_s;-\omega_3,\omega_2,\omega_1)$. These two terms are representative of two general classes of terms found in the expression for $\chi^{(3)}$; those involving only exciton states as in (a) and those involving both exciton and biexciton states as in (b). In Eq. (5.26), R_1 belongs to class (a) while the remaining terms (R_2–R_5) belong to class (b).

$$\chi^{(3)}(-\omega_s;\omega_3,\omega_2,\omega_1) = 8N^2\mu^4 \sum_p \frac{\omega(0)}{[\omega_1+\omega_2+\omega_3+i(N\gamma/2)]^2-\omega(0)^2} \frac{1}{\omega_1+\omega_2+iN\gamma} \frac{\omega_1+iN\gamma/2}{[\omega_1+i(N\gamma/2)]^2-\omega(0)^2}$$
$$+ 8N(N-1)\mu^4 \sum_p \sum_{q=1,3,5,\ldots}^{N-2} I_q \frac{[\omega(0)-\Omega(0,q)]}{\{\omega_1+\omega_2+\omega_3+i[\Gamma(0,q)+N\gamma/2]\}^2-[\omega(0)-\Omega(0,q)]^2}$$
$$\times \frac{1}{\omega_1+\omega_2+iN\gamma} \frac{\omega_1+i(N\gamma/2)}{[\omega_1+i(N\gamma/2)]^2-\omega(0)^2}$$
$$- 2N(N-1)\mu^4 \sum_p \sum_{q=1,3,5,\ldots}^{N-2} I_q \left\{ \frac{1}{\omega_1+\omega_2+\omega_3+\omega(0)-\Omega(0,q)+i[\Gamma(0,q)+N\gamma/2]} \right.$$

$$-\frac{1}{\omega_1+\omega_2+\omega_3-\omega(0)+i(N\gamma/2)}\Bigg]$$
$$\times\frac{1}{\omega_1+\omega_2-\Omega(0,q)+i\Gamma(0,q)}\frac{1}{\omega_1-\omega(0)+iN\gamma/2}$$
$$+2N(N-1)\mu^4\sum_p\sum_{q=1,3,5,\ldots}^{N-2}I_q\Bigg[\frac{1}{\omega_1+\omega_2+\omega_3-\omega(0)+\Omega(0,q)+i[\Gamma(0,q)+N\gamma/2]}$$
$$-\frac{1}{\omega_1+\omega_2+\omega_3+\omega(0)+i(N\gamma/2)}\Bigg]$$
$$\times\frac{1}{\omega_1+\omega_2+\Omega(0,q)+i\Gamma(0,q)}\frac{1}{\omega_1+\omega(0)+i(N\gamma/2)}\ . \tag{4.11}$$

In this expression the dimensionless weighting factors I_q are given by

$$I_q=\frac{2}{N(N-1)}\cot^2\frac{q\pi}{2N}\ , \tag{4.12}$$

and are normalized according to

$$\sum_{q=1,3,5,\ldots}^{N-2}I_q=1\ . \tag{4.13}$$

I_q is related to the exciton–qth-biexciton transition dipole moment, given by

$$\langle\langle b(0)|\mathcal{V}|B(0,q)\rangle\rangle=\mu[2(N-1)I_q]^{1/2}\ . \tag{4.14}$$

[We should point out that Eq. (4.11) is applicable for odd values of N which, in addition, satisfy $N\geq 5$. For $N=3$, Eq. (4.11) is still valid provided one uses $I_1=1$, $\Omega(0,q)=2\omega_0+2V$, and $\Gamma(0,1)=2\gamma$.] The first term in Eq. (4.11) represents the contribution to $\chi^{(3)}$ from all interaction processes which involve only the exciton state, such as the one depicted in Fig. 1(a). The remaining terms involve the biexciton states [Fig. 1(b)]; the second term is resonantly enhanced for processes which involve biexciton formation through single-photon absorption from an initial exciton population, while the last two terms involve biexciton formation via direct two-photon absorption.

The aggregate size N appears in Eq. (4.11) as N^2 and $N(N-1)$ prefactors, arising from the enhanced exciton and exciton-biexciton transition dipole moments, respectively, and in the imaginary parts of all three denominators, due to the superradiant radiative decay of the exciton and biexciton states. Therefore, the scaling of $\chi^{(3)}$ with size depends on the particular nonlinear technique, for example, $\chi^{(3)}$ for degenerate four-wave mixing will have a distinctly different N dependence than $\chi^{(3)}$ for third-harmonic generation. Our new expression for $\chi^{(3)}$ [Eq. (4.11)] will be analyzed in detail in Secs. VI and VII for two specific four-wave mixing techniques. This will be done following the incorporation of pure dephasing in Sec. V. There is, however, one very general limiting case which is the most important from a technological viewpoint, i.e., when all three fields are far off resonance ($\omega_1\pm\omega_2\pm\omega_3\pm\omega_0\gg V$, $\omega_1\pm\omega_2\gg N\gamma$, and $\omega_1\pm\omega_0\gg V$). It was predicted in this case that $\chi^{(3)}$ would vanish because the two-level systems behave as harmonic oscillators.[24] In order to explore this point we take the off-resonance limit of our $\chi^{(3)}$. This is done by substituting the approximations $\omega(0)\approx\omega_0$ and $\Omega(0,q)\approx 2\omega_0$ into Eq. (4.11) and neglecting the superradiant contribution in the denominators. It then appears, at first glance, that (when N is large) $\chi^{(3)}$ is enhanced by a factor of N^2. Since, for N monomers, $\chi^{(3)}\sim N$, we are led to the conclusion that the effect of aggregation, in this limit, is to enhance $\chi^{(3)}$ by a factor of N. This conclusion is, however, false. When all the terms in $\chi^{(3)}$ [Eq. (4.11)] are added in this limit we get

$$\chi^{(3)}(-\omega_s;\omega_3,\omega_2,\omega_1)$$
$$=8N\mu^4\sum_p\frac{\omega_0}{(\omega_1+\omega_2+\omega_3)^2-\omega_0^2}\frac{1}{\omega_1+\omega_2}\frac{\omega_1}{\omega_1^2-\omega_0^2}\ . \tag{4.15}$$

The N^2 parts of Eq. (4.11) beautifully cancel due to an interference between the first and second terms of Eq. (4.11). In addition, the third and fourth terms exactly cancel, leaving the monomer result given by Eq. (4.15). This is understandable since, under these far-off-resonant conditions, the material response is very rapid and the molecules will not have time to interact with each other and establish aggregate properties. It is also important to note that the biexciton states, which contribute the last three terms in Eq. (4.11), are necessary to arrive at this result. It is not appropriate to treat the aggregate as a two-level system with an enhanced oscillator strength and radiative rate.

V. HOMOGENEOUS DEPHASING

Molecular aggregates in the condensed phase are subject to medium-induced fluctuations which act to destroy the intermolecular phase relationships. If the fluctuations occur on a time scale much shorter than that of the excitation dynamics, they result in homogeneous dephasing. In this section we recalculate the expression for $\chi^{(3)}$ when this homogeneous dephasing is taken into account.

Homogeneous dephasing is introduced by assuming that each molecular electronic frequency is undergoing rapid fluctuations:

$$\omega_n(t)=\omega_0+\delta\omega_n(t)\ , \tag{5.1}$$

with

$$\langle\delta\omega_n(t)\rangle=0\ , \tag{5.2}$$

and

$$\langle \delta\omega_n(t)\delta\omega_{n'}(0)\rangle = \hat{\Gamma}\delta(t)\delta_{n,n'} . \tag{5.3}$$

Here $\langle \cdots \rangle$ denotes an ensemble average over the bath, and it is assumed that fluctuations on different molecules are uncorrelated. $\delta\omega(t)$ is taken to be a stochastic Gaussian-Markov process. This model was introduced by Haken and Strobl to describe exciton transport in solids.[25] The *ensemble-averaged* density-matrix (σ) equation of motion in the absence of the external field satisfies the following equation:

$$\frac{d}{dt}\sigma(t) = -i(L_0 + L')\sigma(t) , \tag{5.4}$$

where $L_0 = L_1 + L_2$ and the matrix elements of L' are

$$\langle\langle b(n)|L'|b(n')\rangle\rangle = -i\frac{\hat{\Gamma}}{2}\delta_{nn'} \tag{5.5a}$$

in the exciton coherence basis set $[|b(n)\rangle\rangle \equiv b_n^\dagger|0\rangle\langle 0|]$,

$$\langle\langle b(n)\bar{b}(m)|L'|b(n')\bar{b}(m')\rangle\rangle = -i(1-\delta_{nm})\hat{\Gamma}\delta_{nn'}\delta_{mm'} \tag{5.5b}$$

in the subspace spanned by the $b_n^\dagger|0\rangle\langle 0|b_m$ basis,

$$\langle\langle B(n,m)|L'|B(n',m')\rangle\rangle = -i\hat{\Gamma}(\delta_{nn'}\delta_{mm'} + \delta_{nm'}\delta_{mn'}) , \tag{5.5c}$$

in the biexciton subspace spanned by $|B(n,m)\rangle\langle 0| \equiv b_n^\dagger b_m^\dagger|0\rangle\langle 0|$, and

$$\langle\langle B(n,m)\bar{b}(l)|L'|B(n',m')\bar{b}(l')\rangle\rangle = -i\left[\frac{3\hat{\Gamma}}{2}(1-\delta_{ml})(1-\delta_{nl}) + \frac{\hat{\Gamma}}{2}\delta_{ml} + \frac{\hat{\Gamma}}{2}\delta_{nl}\right][\delta_{ll'}(\delta_{nn'}\delta_{mm'} + \delta_{nm'}\delta_{mn'})] , \tag{5.5d}$$

in the biexciton-exciton coherence space, spanned by $|B(n,m)\rangle\langle b(l)| \equiv b_n^\dagger b_m^\dagger|0\rangle\langle 0|b_l$.

In order to evaluate $\chi^{(3)}$, we need to recalculate the Green functions when L' is taken into account:

$$\mathcal{G}(\omega) = \frac{1}{\omega - L_0 - L'} . \tag{5.6}$$

This is most easily done for the single-exciton propagator

$$\langle\langle b(0)|\mathcal{G}(\omega)|b(0)\rangle\rangle ,$$

which describes the evolution of the system after a single interaction with the applied field. Since $L'|b(0)\rangle\rangle = -i(\hat{\Gamma}/2)|b(0)\rangle\rangle$ we have

$$\langle\langle b(0)|\mathcal{G}(\omega)|b(0)\rangle\rangle = \frac{1}{\omega + \omega(0) + i(N\gamma/2 + \hat{\Gamma}/2)} , \tag{5.7}$$

and the dephasing rate simply enhances the overall exciton coherence decay.

The effect of homogeneous dephasing on the two-photon Green functions is not as straightforward to evaluate. We first note that L', like L_1, cannot couple two operators with different numbers of excitations on the right- and the left-hand sides, for example, $|b(0)b(0)\rangle\rangle$ does not couple to $|b(0)\rangle\rangle$. The two-photon Green function can be of three types: (a) the biexciton propagator, (b) the exciton-population propagator, or (c) the ground-state propagator. In the first case the inclusion of homogeneous dephasing is treated in the same way as the exciton propagator (the single-photon Green function). This is because we have $L'|B(k,q)\rangle\rangle = -i\hat{\Gamma}|B(k,q)\rangle\rangle$ and therefore

$$\langle\langle B(k,q)|\mathcal{G}(\omega)|B(k,q)\rangle\rangle = \frac{1}{\omega + \Omega(k,q) + i[\Gamma(k,q) + \hat{\Gamma}]} . \tag{5.8}$$

Because $|b(k)\bar{b}(k')\rangle\rangle$ is not an eigenfunction of L',

$$\langle\langle b(k)\bar{b}(k')|L'|b(k'')\bar{b}(k''')\rangle\rangle = \hat{\Gamma}(\delta_{k,k'''}\delta_{k',k''} - 1/N) , \tag{5.9}$$

we cannot simply add $\hat{\Gamma}$ to the superradiant decay rate $N\gamma$ in the exciton-population propagator. However, L' is diagonal in the basis set $|A(k,s)\rangle\rangle$ defined by[37]

$$|A(k,s)\rangle\rangle = N^{-1/2}\sum_r \exp\left[\frac{i2\pi kr}{N}\right] \times b_{r-s/2}^\dagger|0\rangle\langle 0|b_{r+s/2} , \tag{5.10}$$

where the indices r and s are defined the same way as in Eq. (3.6). This basis set is orthonormal:

$$\langle\langle A(k',s')|A(k,s)\rangle\rangle = \delta_{s,s'}\delta_{k,k'} . \tag{5.11}$$

The matrix elements of L' in the new basis set are

$$\langle\langle A(k',s')|L'|A(k,s)\rangle\rangle = -i\hat{\Gamma}\delta_{k,k'}\delta_{s,s'}(1-\delta_{s,0}) . \tag{5.12}$$

L' is diagonal with all diagonal elements within a $\mathbf{k}$ subspace equal, except for the population term $\langle\langle A(k,0)|L'|A(k,0)\rangle\rangle$, which is equal to zero. This is because homogeneous dephasing induces a coherence decay but does not affect the populations. The null diagonal element can be treated like a single impurity and we can therefore make use of single-impurity scattering theory[37,38] to evaluate the Green function. According to the Dyson equation, the exact Green function $\mathcal{G}(\omega)$ is related to the unperturbed Green function $\mathcal{G}^0(\omega)$ by

$$\mathcal{G}(\omega) = \mathcal{G}^0(\omega) + \mathcal{G}^0(\omega)T(\omega)\mathcal{G}^0(\omega) , \tag{5.13}$$

where, because of the translational invariance, Eq. (5.13) is separately true in each subspace spanned by $|A(k,s)\rangle\rangle$, i.e., the Green function is diagonal in k. The T matrix $T(\omega)$ is given by

$$T(\omega) = \frac{i\hat{\Gamma}|A(k,0)\rangle\rangle\langle\langle A(k,0)|}{1 - i\hat{\Gamma}Q(k,\omega)} , \tag{5.14}$$

with $Q(k,\omega)$ defined as

$$Q(k,\omega)=\langle\langle A(k,0)|\mathcal{G}^0(\omega)|A(k,0)\rangle\rangle . \tag{5.15}$$

By taking matrix elements of Eq. (5.13) we obtain

$$\langle\langle b(0)\bar{b}(0)|\mathcal{G}(\omega)|b(0)\bar{b}(0)\rangle\rangle = \frac{1}{\omega+iN\gamma+i\hat{\Gamma}}+N^{-1}\frac{i\hat{\Gamma}(\omega+i\hat{\Gamma})}{(\omega+i\gamma^+)(\omega+i\gamma^-)} \tag{5.16}$$

for the exciton-population propagator. The damping rates γ^+ and γ^- are defined as

$$\gamma^{\pm}=\frac{(N\gamma+\hat{\Gamma})}{2}\pm\tfrac{1}{2}[(\hat{\Gamma}+N\gamma)^2-4\gamma\hat{\Gamma}]^{1/2} . \tag{5.17}$$

When $\hat{\Gamma}=0$ Eq. (5.16) correctly reduces to Eq. (4.9b)—the exciton propagator without dephasing. There is also a coupling mechanism which transfers population from the $k=0$ exciton to $k\neq 0$ excitons:

$$\langle\langle b(k)\bar{b}(k')|\mathcal{G}(\omega)|b(0)\bar{b}(0)\rangle\rangle = N^{-1}\frac{i\hat{\Gamma}}{(\omega+i\gamma^+)(\omega+i\gamma^-)} . \tag{5.18}$$

For the three-photon Green function, the only propagator which is not straightforward to evaluate is the exciton-biexciton Green function. For this case the influence of homogeneous dephasing cannot be calculated exactly; however, we can use perturbation theory to get an approximate result. We begin by writing the matrix elements of L' in the exciton-biexciton basis set:

$$\langle\langle B(k_1,q_1)\bar{b}(k)|L'|B(k_2,q_2)\bar{b}(k')\rangle\rangle=\frac{-8\hat{\Gamma}}{N^2}\sum_{s=1}^{(N-1)/2}\sin\left[\frac{\pi q_1 s}{N}\right]\sin\left[\frac{\pi q_2 s}{N}\right]\cos\left[\frac{\pi(k-k')s}{N}\right]\delta_{k_1-k_2,k-k'} \tag{5.19}$$

for off-diagonal elements, and equal to $3\hat{\Gamma}/2-2\hat{\Gamma}/N$ for diagonal elements. These diagonal elements are the first-order (complex) energy correction. This is a good approximation to the exact energy correction when the magnitude of the off-diagonal elements is less than the differences in the real, unperturbed, zeroth-order energy values given by

$$E(k,q;k')\equiv\Omega(k,q)-\omega(k')=\omega_0+4V\cos\left[\frac{\pi k}{N}\right]\cos\left[\frac{\pi q}{N}\right]-2V\cos\left[\frac{2\pi k'}{N}\right] . \tag{5.20}$$

Now, the magnitude of the off-diagonal perturbations given by Eq. (5.19) cannot exceed $4\Gamma/N$ and the average energy-level difference is of the order V/N^3. Therefore the first-order correction is good if

$$N^2\frac{\hat{\Gamma}}{V}\ll 1 . \tag{5.21}$$

The approximate exciton-biexciton coherence propagator can then be written as

$$\langle\langle B(k_1,q_1)\bar{b}(k)|\mathcal{G}(\omega)|B(k_2,q_2)\bar{b}(k')\rangle\rangle\cong\frac{\delta_{k_1,k_2}\delta_{q_1,q_2}\delta_{k,k'}}{E(k_1,q_1;k)+i[(N\gamma/2)\delta_{k,0}+\Gamma(k_1,q_1)+3\hat{\Gamma}/2-2\hat{\Gamma}/N]} . \tag{5.22}$$

Using the Green-function matrix elements derived above, we can now calculate the third-order susceptibility with homogeneous dephasing satisfying condition (5.21):

$$\begin{aligned}\chi^{(3)}(-\omega_s;\omega_3,\omega_2,\omega_1)&=8N^2\mu^4\sum_p\frac{\omega(0)}{(\omega_1+\omega_2+\omega_3+iN\gamma/2+i\hat{\Gamma}/2)^2-\omega(0)^2}\\&\times\frac{2(\omega_1+\omega_2+i\gamma^+)(\omega_1+\omega_2+i\gamma^-)+[i(N+1)/N]\hat{\Gamma}(\omega_1+\omega_2+i\hat{\Gamma})-(N-1)\gamma\hat{\Gamma}}{(\omega_1+\omega_2+iN\gamma+i\hat{\Gamma})(\omega_1+\omega_2+i\gamma^+)(\omega_1+\omega_2+i\gamma^-)}\\&\times\frac{\omega_1+i(N\gamma/2+\hat{\Gamma}/2)}{[\omega_1+i(N\gamma/2+\hat{\Gamma}/2)]^2-\omega(0)^2}\\&+8N(N-1)\mu^4\sum_p\sum_{q=1,3,5,\ldots}^{N-2}I_q\frac{[\omega(0)-\Omega(0,q)]}{\{\omega_1+\omega_2+\omega_3+i[\Gamma(0,q)+N\gamma/2+(\frac{3}{2}-2/N)\hat{\Gamma}]\}^2-[\omega(0)-\Omega(0),q)]^2}\\&\times\frac{(\omega_1+\omega_2+i\gamma^+)(\omega_1+\omega_2+i\gamma^-)+i(\hat{\Gamma}/N)(\omega_1+\omega_2+i\hat{\Gamma})}{\omega_1+\omega_2+iN\gamma+i\hat{\Gamma})(\omega_1+\omega_2+i\gamma^+)(\omega_1+\omega_2+i\gamma^-)}\frac{\omega_1+i(N\gamma/2+\hat{\Gamma}/2)}{[\omega_1+i(N\gamma/2+\hat{\Gamma}/2)]^2-\omega(0)^2}\end{aligned}$$

$$-2N(N-1)\mu^4\sum_p\sum_{q=1,3,5,\ldots}^{N-2} I_q\left[\frac{1}{\omega_1+\omega_2+\omega_3+\omega(0)-\Omega(0,q)+i[\Gamma(0,q)+N\gamma/2+(\frac{3}{2}-2/N)\hat{\Gamma}]}\right.$$
$$\left.-\frac{1}{\omega_1+\omega_2+\omega_3-\omega(0)+i(N\gamma/2+\hat{\Gamma}/2)}\right]$$
$$\times\frac{1}{\omega_1+\omega_2-\Omega(0,q)+i[\Gamma(0,q)+\hat{\Gamma}]}\frac{1}{\omega_1-\omega(0)+i(N\gamma/2+\hat{\Gamma}/2)}$$
$$+2N(N-1)\mu^4\sum_p\sum_{q=1,3,5,\ldots}^{N-2} I_q\left[\frac{1}{\omega_1+\omega_2+\omega_3-\omega(0)+\Omega(0,q)+i[\Gamma(0,q)+N\gamma/2+(\frac{3}{2}-2/N)\hat{\Gamma}]}\right.$$
$$\left.-\frac{1}{\omega_1+\omega_2+\omega_3+\omega(0)+i(N\gamma/2+\hat{\Gamma}/2)}\right]$$
$$\times\frac{1}{\omega_1+\omega_2+\Omega(0,q)+i[\Gamma(0,q)+\hat{\Gamma}]}\frac{1}{\omega_1+\omega(0)+i(N\gamma/2+\hat{\Gamma}/2)}$$
$$+4N(N-1)\mu^4\sum_p\sum_{k\neq 0}^{N-1}\sum_{q=1,3,5,\ldots}^{N-2} I_{k,q}\frac{\omega(k)-\Omega(k,q)}{\{\omega_1+\omega_2+\omega_3+i[\Gamma(k,q)+(\frac{3}{2}-2/N)\hat{\Gamma}]\}^2-[\omega(k)-\Omega(k,q)]^2}$$
$$\times\frac{i\hat{\Gamma}}{(\omega_1+\omega_2+i\gamma^+)(\omega_1+\omega_2+i\gamma^-)}\frac{\omega_1+i(N\gamma/2+\hat{\Gamma}/2)}{[\omega_1+i(N\gamma/2+\hat{\Gamma}/2)]^2-\omega(0)^2}\ , \tag{5.23}$$

where the I_q were defined in Eq. (4.12) and $I_{k,q}$ are defined as

$$I_{k,q}=\frac{1}{N^2(N-1)}\left[\cot\left[\frac{(q-k)\pi}{2N}\right]+\cot\left[\frac{(q+k)\pi}{2N}\right]\right]^2, \tag{5.24}$$

and are normalized according to

$$\sum_{k=0}^{N-1}\sum_{q\ \text{odd}}^{N-2} I_{k,q}=1\ . \tag{5.25}$$

For the subsequent analysis we rewrite Eq. (5.23) in the form

$$\chi^{(3)}(-\omega_s;\omega_3,\omega_2,\omega_1)=\sum_p\sum_{j=1}^{5} R_j(\omega_1+\omega_2+\omega_3,\omega_1+\omega_2,\omega_1)\ , \tag{5.26}$$

where R_j, $j=1,\ldots,5$, correspond, respectively, to the five terms in Eq. (5.23). The general expression for $\chi^{(3)}$ in Eq. (5.23) is too complex to draw general conclusions. In the next two sections we will focus on two specific $\chi^{(3)}$ spectroscopies and analyze them in detail.

VI. PHASE-CONJUGATE FOUR-WAVE MIXING

As established earlier, the size dependence of $\chi^{(3)}$ varies with the particular nonlinear technique (singly, doubly, or triply resonant) because of the N-dependent superradiant damping rates in the three denominators. In this section we specifically treat phase-conjugate four-wave-mixing spectroscopy and analyze its dependence on N, the pure dephasing rate $\hat{\Gamma}$, and the laser frequency detuning. We also include inhomogeneous broadening perturbatively.

In phase-conjugate DFWM, two pump beams with frequency ω_1 counterpropagate in a nonlinear medium ($\mathbf{k}_3=-\mathbf{k}_1$), with the probe beam (frequency ω_2, wave vector $\mathbf{k}_2$) entering at some arbitrary angle. A phase-conjugate signal with an intensity proportional to $|\chi^{(3)}|^2$ is generated in the $\mathbf{k}_s=\mathbf{k}_1+\mathbf{k}_3-\mathbf{k}_2=-\mathbf{k}_2$ direction with a frequency equal to $2\omega_1-\omega_2$. In this particular arrangement we have

$$\chi^{(3)}(-\omega_s;\omega_1,-\omega_2,\omega_1)=\sum_{j=1}^{5} 2R_j(2\omega_1-\omega_2,\omega_1-\omega_2,\omega_1)$$
$$+R_j(2\omega_1-\omega_2,\omega_1-\omega_2,-\omega_2)$$
$$+2R_j(2\omega_1-\omega_2,2\omega_1,\omega_1)\ , \tag{6.1}$$

where R_j were defined in Eq. (5.26) and the factor of 2 in the first and third terms arises from the possibility of absorbing either one of the pump-beam photons ($\mathbf{k}_1$ or $-\mathbf{k}_1$). In DFWM, the pump frequency ω_1 is held fixed while the probe-beam frequency is scanned over a narrow frequency interval centered at ω_1. In this section we treat two cases. In the first case the pump beams are tuned to the exciton absorption maximum, $\omega_1=\omega(0)=\omega_0+2V$. In the second case, the pump beams are detuned by at least an exciton bandwidth from the $k=0$ exciton absorption maximum, $\omega_1-\omega(0)>V$, and ω_2 is scanned over a narrow frequency interval centered at ω_1.

A. Case A: Resonant DFWM

In the resonant case where $\omega_1=\omega(0)$, the dominant terms in $\chi^{(3)}$ are the exciton terms $[R_1(2\omega_1-\omega_2,\omega_1-\omega_2,\omega_1)$ and $R_1(2\omega_1-\omega_2,\omega_1-\omega_2,-\omega_2)]$ in Eq. (6.1), since only these terms are triply resonant when $\omega_2\approx\omega(0)$. All other terms are at best doubly resonant. For example, $R_2(2\omega_1-\omega_2,\omega_1-\omega_2,\omega_1)$ is resonantly enhanced in the one- and two-photon Green functions when $\omega_2=\omega(0)$ but not in the three-photon Green function. The last term in Eq. (6.1) is resonantly enhanced in $R_3(2\omega_1-\omega_2,2\omega_1,\omega_1)$ representing biexciton excitation via two-photon absorption. However, the process is only doubly resonant since the two-photon Green function is not resonant when $2\omega_1-\Omega(0,q)\gg\hat{\Gamma}+\Gamma(0,q)$. This difference is called the biexciton binding energy; substituting $\Omega(0,q)=2\omega_0+4V\cos(\pi/N)$ and $\omega_1=\omega(0)$ into the previous condition yields

$$|4V[\cos(\pi/N)-1]|\gg\hat{\Gamma}+\Gamma(0,q)\ . \tag{6.2}$$

Therefore the biexciton binding energy $[\Omega(0,q)-2\omega(0)]$ must be much greater than the superradiant decay rate plus the pure dephasing rate in order to justify the neglect of two-photon absorption $[R_3(2\omega_1-\omega_2,2\omega_1,\omega_1)]$. Including only triply resonant terms, Eq. (6.1) becomes

$$\chi^{(3)}(-\omega_s;\omega_1,-\omega_2,\omega_1)=2R_1(2\omega_1-\omega_2,\omega_1-\omega_2,\omega_1)+R_1(2\omega_1-\omega_2,\omega_1-\omega_2,-\omega_2). \tag{6.3}$$

In this case, the aggregate can be modeled as a two-level system consisting of the ground state and the exciton state, with an enhanced transition dipole moment.

We shall denote the pump-laser detuning from the exciton absorption line center as $\Delta\omega_1\equiv\omega_1-\omega(0)$. In order not to excite the biexciton state with two detuned pump-beam photons we require that

$$|4V[\cos(\pi/N)-1]+2\Delta\omega_1|\gg\hat{\Gamma}+\Gamma(0,q)\ , \tag{6.4}$$

which is condition (6.2) modified to include the detuning.

The inclusion of inhomogeneous broadening makes the resulting expression for $\chi^{(3)}$ much more complicated; in general we need to numerically invert a large coupling matrix (order $N^3\times N^3$) so that a simple analytical expression is not available. However, if the inhomogeneous broadening is sufficiently small it can be incorporated perturbatively. This is done as follows. According to the definition of inhomogeneous broadening, each molecule has a unique transition frequency which is detuned from ω_0 by an amount $\delta\omega_n$. We assume $\delta\omega_n$ are independent Gaussian random variables with variance σ^2 so that the monomer absorption spectrum is Gaussian. A simple first-order perturbative treatment, valid when[5,11]

$$N^3(\sigma/V)^2\ll 8\pi^4\ , \tag{6.5}$$

yields the following first-order energy correction to the ($k=0$) exciton energy of the aggregate:

$$\delta\omega_a=\frac{1}{N}\sum_{n=1}^{N}\delta\omega_n\ . \tag{6.6}$$

$\delta\omega_a$ is also a normally distributed random variable but with variance σ^2/N. Thus, the width of the exciton absorption spectrum is less than that of the monomer. This reduction is a result of the central limit theorem and can be interpreted as motional narrowing.[5] When condition (6.5) holds, the exciton-biexciton basis set is approximately the eigenbasis, and the expression for $\chi^{(3)}$ given by Eq. (5.23) is valid for a particular distribution of $\delta\omega_n$ provided the first-order corrections to $\omega(k)$ and $\Omega(k,q)$ are included. [For example, we replace the exciton energy $\omega(0)$ by $\omega(0)+\delta\omega_a$ in $R_1(2\omega_1-\omega_2,\omega_1-\omega_2,\omega_1)$ and $R_1(2\omega_1-\omega_2,\omega_1-\omega_2,-\omega_2)$.] We must then average $\chi^{(3)}$ over all values of $\delta\omega_a$ in the Gaussian inhomogeneous line shape. In order to continue to ignore two-photon biexciton absorption we require, as before, the two-photon Green function in $R_3(2\omega_1-\omega_2,2\omega_1,\omega_1)$ to be nonresonant. Since the shift in biexciton transition frequency is equal to $(2/N)\sum_{n=1}^{N}\delta\omega_n$, we require that

$$\left|4V[\cos(\pi/N)-1]-\frac{2}{N}\sum_{n=1}^{N}\delta\omega_n\right|\gg\hat{\Gamma}+\Gamma(0,q)\ . \tag{6.7}$$

In order to characterize the scaling of DFWM with size, we evaluate the total number of photons per second emitted in the direction $-\mathbf{k}_2$ integrated over the frequency range $\omega_1-\omega_2$. This quantity (apart from some geometric proportionality constants) will be denoted as $S(N,\hat{\Gamma},\Delta\omega_1)$, which is also a strong function of the homogeneous dephasing rate $\hat{\Gamma}$ and the detuning $\Delta\omega_1$:

$$S(N,\hat{\Gamma},\Delta\omega_1)=\mu^{-8}\int_{-\infty}^{\infty}|\chi^{(3)}[-(2\omega_1-\omega_2);\omega_1,-\omega_2,\omega_1]|^2d\omega_2 \tag{6.8}$$

We have plotted $S(N,\hat{\Gamma},\Delta\omega_1)$ versus N for several values of $\hat{\Gamma}$ and pump-laser detuning $\Delta\omega_1$ in Figs. 2(a)–2(d). As is evident the aggregate size dependence is not a simple function N. Two general observations can be made when the pump beams are tuned to the peak in the exciton absorption spectrum ($\Delta\omega_1=0$). When superradiance dominates homogeneous dephasing ($N\gamma\gg\hat{\Gamma}$), $S(N,\hat{\Gamma},\Delta\omega_1)$ is a monotonic *decreasing* function of N; in the opposite limit ($\hat{\Gamma}\gg N\gamma$), $S(N,\hat{\Gamma},\Delta\omega_1)$ is a monotonic *increasing* function of N. Simple analytical expressions are easily derivable in these two limits. To analyze the small de-

phasing regime we set $\hat{\Gamma}=0$ and obtain

$$S(N,0,0)=2\pi\frac{704}{9\gamma^5}N^{-1}\ , \tag{6.9}$$

which is the N dependence clearly displayed in Fig. 2(a). In this case $\chi^{(3)}$ is actually degraded with size. In the opposite limit $\hat{\Gamma}\gg N\gamma$ we set $N\gamma=0$ and obtain

$$S(N,\hat{\Gamma},0)=2\pi\frac{72}{\hat{\Gamma}^4\gamma}N^4\ , \tag{6.10}$$

which is the behavior seen in Fig. 2(d). This case shows enhancement above the monomer dependence ($S_{\rm mon}\propto N^2$). This is quite interesting since one would expect the monomer result when the dephasing $\hat{\Gamma}$ is large. In this limit, the dephasing destroys the superradiance but does not affect the eigenstates, determined by the real part of the coupling V. Therefore, Eq. (6.10) is characteristic of an exciton with a nonsuperradiant fluorescence rate.

The effect of a small pump-beam detuning [within the limit set by condition (6.4)] can also be worked out in these two limits. When $\hat{\Gamma}\gg N\gamma,\Delta\omega_1$, the detuning is unimportant and Eq. (6.10) is still valid. This can be seen in Fig. 2(d), where the variation with N is independent of the magnitude of $\Delta\omega_1$. In the limit $\Delta\omega_1\gg\hat{\Gamma}\gg N\gamma$ the N^4 dependence also remains:

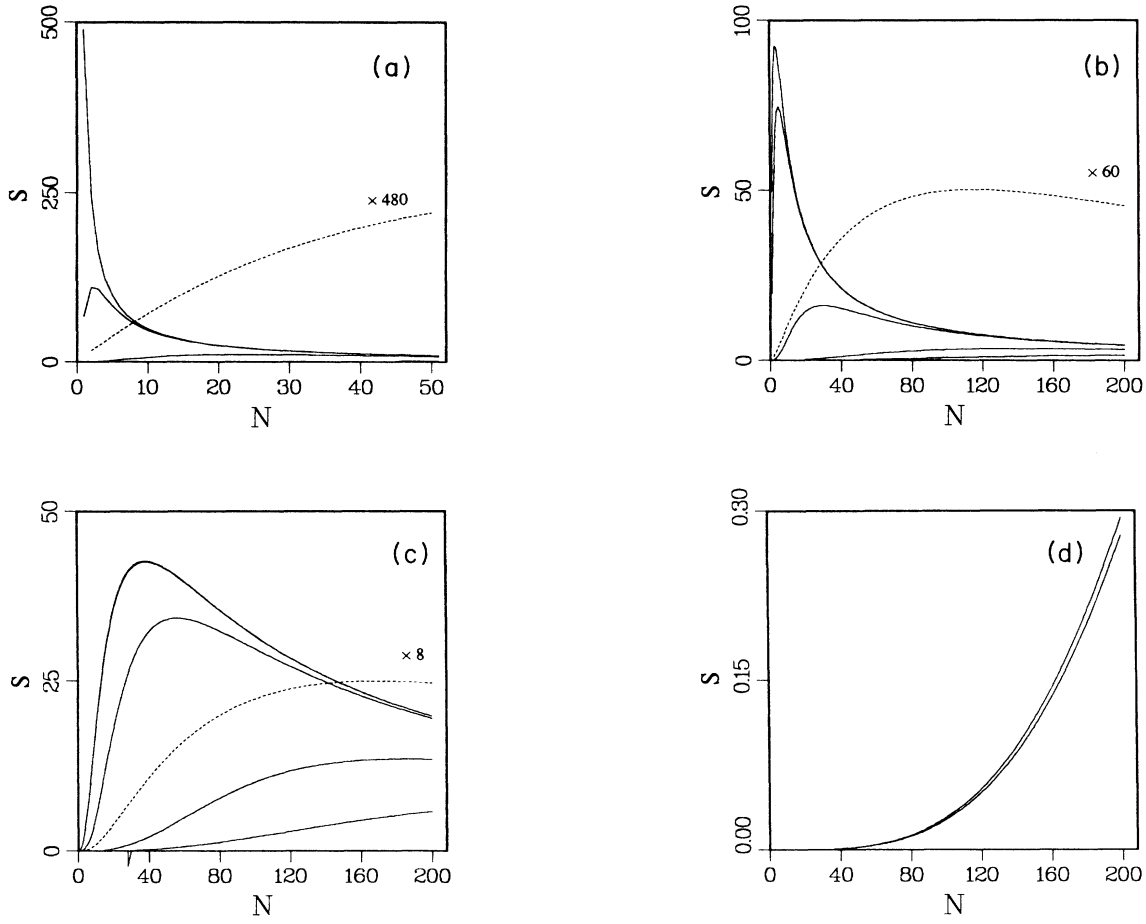

FIG. 2. $S(N,\hat{\Gamma},\Delta\omega_1)$ vs aggregate size N for several values of pump-laser detuning $\Delta\omega_1$ found by integrating $|\chi^{(3)}(-2\omega_1+\omega_2;\omega_1,-\omega_2,\omega_1)|^2$ over ω_2 using $\chi^{(3)}$ from Eq. (5.23) for a phase-conjugate DFWM configuration. The pump-beam frequency is held constant at $\omega_1=\omega_0+2V$. Each panel contains several curves corresponding to different detunings $\Delta\omega_1/\gamma$. In all cases S decreases as $\Delta\omega_1/\gamma$ increases. (a) $\hat{\Gamma}/\gamma=0.01$ and $\Delta\omega_1/\gamma=0$, 1, and 10. (b) $\hat{\Gamma}/\gamma=1.0$ and $\Delta\omega_1/\gamma=0$, 1, 10, 50, and 100. (c) $\hat{\Gamma}/\gamma=10$ and $\Delta\omega_1/\gamma=0$, 1, 10, 50, and 100 ($\Delta\omega_L/\gamma=0$ coincides with $\Delta\omega_1/\gamma=1$). (d) $\hat{\Gamma}/\gamma=1000$ and $\Delta\omega_1/\gamma=0$ and 100. The dashed curves in (a)–(c) represent an average over the inhomogeneous broadening with $\sigma=100\gamma$ within the motional narrowing regime. $\chi^{(3)}$ was calculated by averaging over 100 values of $\Delta\omega_1$ from -200γ to 200γ. The dashed curves are displayed on an expanded scale, as indicated.

$$S(N,\hat{\Gamma},\Delta\omega_1)=\pi\frac{1}{\Delta\omega_1^4\gamma}N^4,\quad \Delta\omega_1\gg\hat{\Gamma}\gg N\gamma\ . \tag{6.11}$$

In the superradiant limit ($\Delta\omega_1\gg N\gamma\gg\hat{\Gamma}$) the variation with N is highly dependent on pump-beam detuning:

$$S(N,0,\Delta\omega_1)=2\pi\frac{45}{\Delta\omega_1^4\gamma}N^3,\quad \Delta\omega_1\gg N\gamma\gg\hat{\Gamma}\ . \tag{6.12}$$

At finite detuning, the $1/N$ dependence changes to an N^3 dependence.

The dashed curves in Figs. 2(a)–2(c) represent the effect of inhomogeneous broadening on the size dependence when conditions (6.4) and (6.5) are satisfied. The curves are a result of averaging $\chi^{(3)}$ over an interval $\Delta\omega_a=-200\gamma$ to 200γ with $\sigma=100\gamma$ for each value of $\omega_1-\omega_2$. Notice that in all cases [and in particular the superradiant limit Fig. 2(a)] S is initially an increasing function of N.

In order to more clearly demonstrate the scaling of the optical nonlinearities with size, we show in Figs. 3(a) and 3(b) the phase-conjugate DFWM spectrum in the case of $\hat{\Gamma}=0$ and $\hat{\Gamma}=10^4\gamma$ for several aggregate sizes. Note that the peak value of $|\chi^{(3)}|^2\sim 1/N^2$ in Fig. 3(b) while $|\chi^{(3)}|^2\sim N^4$ in Fig. 3(a). Also, when $\hat{\Gamma}\ll N\gamma$ the superradiant damping rates in the denominators of the single-, double-, and triple-photon Green functions in $R_1(2\omega_1-\omega_2,\omega_1-\omega_2,\omega_1)$ and $R_1(2\omega_1-\omega_2,\ \omega_1-\omega_2,-\omega_2)$ combine to yield a spectrum with a full width at half maximum (FWHM) that depends linearly on N. Hence, the width of the phase-conjugate DFWM spectrum is an accurate measure of aggregate size. This is clearly seen in Fig. 4 where we display the same spectra as in Fig. 3(a) except that the peak heights are normalized to unity. When $\hat{\Gamma}\gg N\gamma$ as in Fig. 3(b), the widths are independent of N.

Homogeneous dephasing has a dramatic effect on the unstructured spectrum of Fig. 4. The addition of an arbitrarily small amount of dephasing $\hat{\Gamma}$ gives rise to a narrow resonance located at the center of the $\hat{\Gamma}=0$ spectrum. In Fig. 5(a) we show normalized spectra for $N=5$, $\Delta\omega_1=0$, and various values of $\hat{\Gamma}$. The narrow spike originates from the two-photon Green function in $R_1(2\omega_1-\omega_2,\omega_1-\omega_2,\omega_1)$ and $R_1(2\omega_1-\omega_2,\omega_1-\omega_2,-\omega_2)$ which, in the limit $\hat{\Gamma}\ll N\gamma$ (where $\gamma^+=N\gamma$ and $\gamma^-=\hat{\Gamma}/N$), becomes

$$\langle\langle b(0)\bar{b}(0)|\mathcal{G}(\omega_1-\omega_2)|b(0)\bar{b}(0)\rangle\rangle = \frac{2}{\omega_1-\omega_2+iN\gamma}+\frac{(N-1)\gamma\hat{\Gamma}}{(N\gamma)^2[\omega_1-\omega_2+i(\hat{\Gamma}/N)]}\ . \tag{6.13}$$

The first term in Eq. (6.13) is simply the superradiant ($\hat{\Gamma}=0$) result. The second term gives the narrow resonance. The height and FWHM of the narrow resonance are equal to $1/\gamma$ and $\hat{\Gamma}/N$, respectively (for $N\gg 1$), so

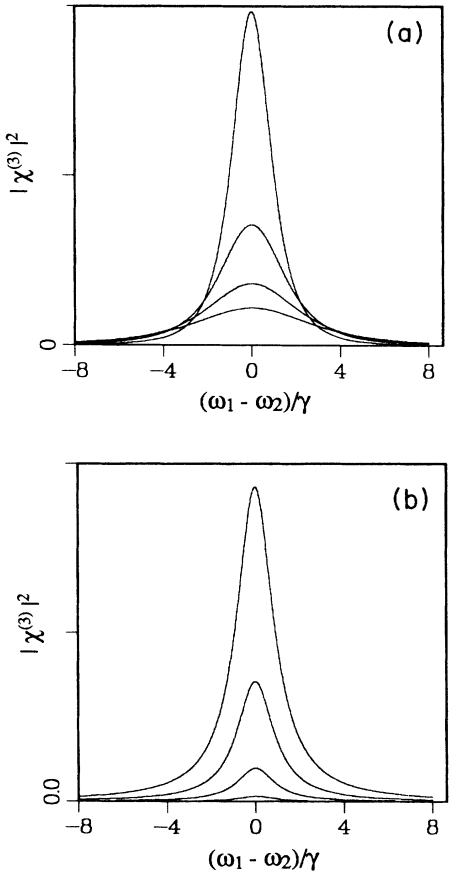

FIG. 3. Phase-conjugate DFWM spectra $|\chi^{(3)}(-2\omega_1+\omega_2;\omega_1,-\omega_2,\omega_1)|^2$ vs $\omega_1-\omega_2$ for several aggregates sizes $N=3$, 5, 7, and 9 with the pump beam tuned to the exciton absorption peak resonance and using the first term of Eq. (5.23) for $\chi^{(3)}$. (a) $\hat{\Gamma}=0$ and increasing aggregate size proceeds from the highest to lowest curve as predicted by Eq. (6.9). (b) $\hat{\Gamma}=10^4$, and the size progression is reversed. $N=9$ now has the largest values of $|\chi^{(3)}|^2$, as is expected from Eq. (6.10).

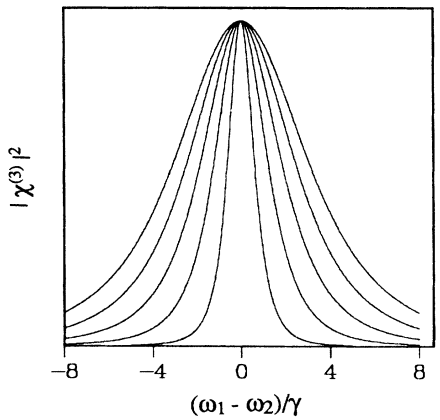

FIG. 4. Phase-conjugate DFWM spectra $|\chi^{(3)}(-2\omega_1+\omega_2;\omega_1,-\omega_2,\omega_1)|^2$ vs $\omega_1-\omega_2$ for several aggregates sizes $N=3$, 5, 7, 9, and 11 in order of increasing linewidth. The curves are normalized to a peak height of unity so that the linewidths can be compared. $\hat{\Gamma}=0$ and the pump-beam frequency is $\omega_1=\omega_0+2V$ ($\Delta\omega_1=0$). Equation (4.11) was used for $\chi^{(3)}$.

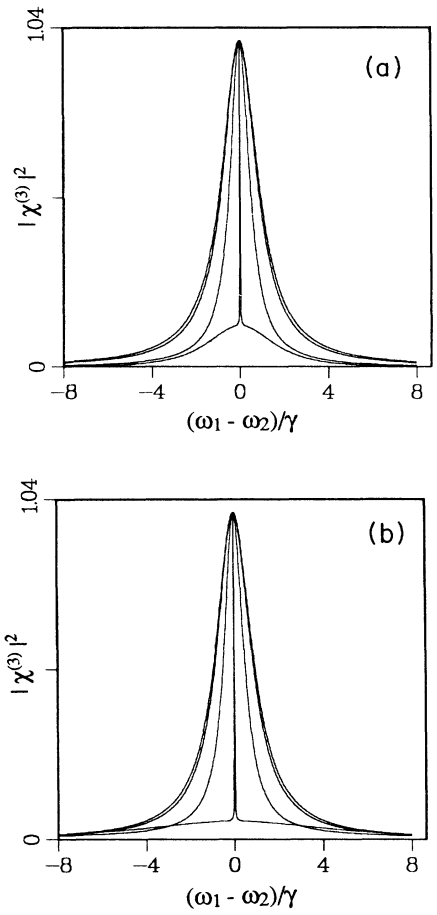

FIG. 5. Phase-conjugate DFWM spectra $|\chi^{(3)}(-2\omega_1+\omega_2;\omega_1,-\omega_2,\omega_1)|^2$ vs $\omega_1-\omega_2$ for $N=5$ and for $\hat{\Gamma}/N\gamma=0.01$, 1, 10, and 100. (a) $\Delta\omega_1=0$ and (b) $\Delta\omega_1=8V$. All curves are normalized to a peak height of unity, and increasing values of $\hat{\Gamma}$ correspond to curves with greater linewidths (at half maximum).

that as $\hat{\Gamma}$ approaches zero, the area correctly goes to zero. The physical origin of this narrow line is based on the property that only the $k=0$ exciton state has a nonzero radiative decay rate and is superradiant. All other exciton states are subradiant. The first interaction with a pump beam directly excites the exciton coherence. After the second interaction (with the probe electric field) the $k=0$ exciton $|b(0)\bar{b}(0)\rangle\rangle$ is populated; during the subsequent evolution period homogeneous dephasing causes a transfer of population, at a rate $\hat{\Gamma}/N$, between $|b(0)\bar{b}(0)\rangle\rangle$ and $|b(k)\bar{b}(k)\rangle\rangle$ where $k\neq 0$. Because these states have no transition dipole moment to the ground state, they cannot radiate and they cannot provide a third interaction with the pump beam to create the phase-conjugate beam. The energy remains "trapped" until it eventually returns to the $k=0$ exciton population, which superradiates and rapidly decays to the ground state. Because of this "slow feeding" to the ground state, the absorption grating persists and scatters the pump beam (third interaction) over a long time equal to $N/\hat{\Gamma}$. This shows up as a narrow resonance in the DFWM spectrum. As the homogeneous dephasing is increased, the trapping become less efficient since the transfer of population is more rapid. In the limit $\hat{\Gamma}\gg N\gamma$, we have $\gamma^+=\gamma$ and $\gamma^-=\hat{\Gamma}$. The two-photon Green function simplifies to

$$\langle\langle b(0)\bar{b}(0)|\mathcal{G}(\omega_1-\omega_2)|b(0)\bar{b}(0)\rangle\rangle=\frac{(N+1)/N}{\omega_1-\omega_2+i\gamma}\ . \tag{6.14}$$

The width of the narrow line converges to γ and the height $(=1/\gamma)$ is unchanged from the $\hat{\Gamma}\ll N\gamma$ result. The area is therefore independent of aggregate size N. This, and the insensitivity to size of the single-photon and three-photon Green functions in $R_1(2\omega_1-\omega_2,\omega_1-\omega_2,\omega_1)$ and $R_1(2\omega_1-\omega_2,\omega_1-\omega_2,-\omega_2)$ when $\hat{\Gamma}\gg N\gamma$, accounts for the N^4 dependence in the quantity S (which is simply due to squaring the N^2 prefactor). The homogeneous dephasing interrupts the radiative decay but does not alter the exciton oscillator strength. Thus the phase-conjugate DFWM resonance is shifted by $2V$ to reflect intermolecular coupling; however, the linewidth is characteristic of a single molecule.

B. Case B: Nonresonant DFWM

We now consider the DFWM experiment with the pump beams far off resonance, $\Delta\omega_1\gg V$. The aggregate size dependence and spectra differ considerably from the resonant case. It is no longer a good approximation to retain only the exciton terms in $\chi^{(3)}$. This is because $R_1(2\omega_1-\omega_2,\omega_1-\omega_2,\omega_1)$, $R_1(2\omega_1-\omega_2,\omega_1-\omega_2,-\omega_2)$, $R_2(2\omega_1-\omega_2,\omega_1-\omega_2,\omega_1)$, $R_2(2\omega_1-\omega_2,\omega_1-\omega_2,-\omega_2)$, $R_5(2\omega_1-\omega_2,\omega_1-\omega_2,\omega_1)$, and $R_5(2\omega_1-\omega_2,\omega_1-\omega_2,-\omega_2)$ are all singly resonant in the two-photon Green function. We can neglect the two-photon absorption terms since they do not contain resonant Green functions.

In the fast-dephasing limit ($\hat{\Gamma}\gg N\gamma$) interference between R_1, R_2, and R_5 *completely* removes the N^2 dependence from $\chi^{(3)}$. The resulting expression (keeping only the dominant, singly resonant terms) becomes

$$\chi^{(3)}(-2\omega_1+\omega_2;\omega_1,-\omega_2,\omega_1)=2N\mu^4\frac{1}{2\omega_1-\omega_2-\omega_0}\frac{2i\hat{\Gamma}}{(\omega_1-\omega_2+i\gamma)(\omega_1-\omega_2+i\hat{\Gamma})}\frac{1}{\omega_1-\omega_0}$$

$$+N\mu^4\frac{1}{2\omega_1-\omega_2-\omega_0}\frac{2i\hat{\Gamma}}{(\omega_1-\omega_2+i\gamma)(\omega_1-\omega_2+i\hat{\Gamma})}\frac{1}{-\omega_2+\omega_0}\ . \tag{6.15}$$

The two-photon Green function can be reduced to $2/(\omega_1-\omega_2+i\gamma)$ since $\hat{\Gamma}\gg\gamma$. When this is substituted back into Eq. (6.15) one recovers the N-monomer result. In the fast dephasing limit $S(N,\hat{\Gamma},\Delta\omega_1)$ is proportional to N^2, which is the monomer result. *When dephasing is dominant (and superradiance is quenched) and the pump beams are off resonance, $\chi^{(3)}$ shows absolutely no enhancement with size above what is expected for N monomers.*

In the superradiant limit the interference between R_1, R_2, and R_5 leads to the two-photon Green function of the form

$$\langle\langle b(0)\bar{b}(0)|\mathcal{G}(\omega_1-\omega_2)|b(0)\bar{b}(0)\rangle\rangle = \frac{2}{(\omega_1-\omega_2+iN\gamma)}+\frac{2(N-1)\gamma\hat{\Gamma}}{(N\gamma)^2[\omega_1-\omega_2+i(\hat{\Gamma}/N)]}, \tag{6.16}$$

where the first term represents the superradiant line shape and the second is the narrow resonance. The complete $\chi^{(3)}$ is obtained by replacing the two-photon Green function in Eq. (6.15) by expression (6.16). Again, the N^2 prefactor in $\chi^{(3)}$ has been reduced to N. It is easy to see that $S(N,\hat{\Gamma},\Delta\omega_1)$ in the superradiant limit is proportional to N [only the superradiant portion in expression (6.16) will contribute when $N\gamma\gg\hat{\Gamma}$] as opposed to $S(N,\hat{\Gamma},\Delta\omega_1)$ in the resonant case which has an N^{-1} dependence [see Eq. (6.9)]. In Fig. 5(b) we show the DFWM spectrum when the pump beams are off resonance ($\Delta\omega_1=8V$). Compared with the on-resonance spectrum, the narrow resonance peak height is an additional factor of 2 larger than the superradiant peak due to the two-photon Green function [compare Eq. (6.16) with Eq. (6.13)]. The superradiant spectrum still appears despite the pump beams being far off resonance. Note, however, that, like the resonant case, the narrow resonance peak height remains $\sim N$ times larger than the superradiant peak height.

VII. PUMP-PROBE SPECTROSCOPY

The phase-conjugate FWM spectra described in the preceding section are dominated by the $k=0$ exciton line shape. The terms leading to the biexciton spectral peaks are doubly resonant at best (when $\Delta\omega_1=0$) and are small in comparison to the (triply resonant) exciton peak. The question arises as to how one could observe biexciton line shapes which are enhanced through a triple resonance in the nonlinear susceptibility. Two standard nonlinear optical techniques will accomplish this: the transient grating experiment and a pump-probe nonlinear absorption experiment. The former measures $|\chi^{(3)}|^2$ while the latter measures $\mathrm{Im}\chi^{(3)}$. In this section we will focus attention on the absorption experiment. A resonant pump beam with frequency ω_1 interacts with the system of aggregates with $\omega_1=\omega_0+2V$. The spectrum is obtained by measuring the absorption of a probe beam as its frequency is tuned through resonance. The change of the probe absorption in the presence of the pump beam is a third-order nonlinear process requiring two interactions with the pump beam and a single interaction with the probe beam. The third-order polarization which causes the absorption change generates an electric field with wave vector $\mathbf{k}_s=\mathbf{k}_1-\mathbf{k}_1+\mathbf{k}_2=\mathbf{k}_2$ and frequency $\omega_2+\omega_1-\omega_1=\omega_2$. The third-order field copropagates with the probe beam and is identical in frequency. The third-order absorption is proportional to $\mathrm{Im}\chi^{(3)}(-\omega_2,-\omega_1,\omega_2,\omega_1)$. Analysis of Eq. (5.23) reveals the possibility of triple resonances in all but R_4. For example, $R_3(\omega_2,\omega_1+\omega_2,\omega_1)$, $R_2(\omega_2,0,\omega_1)$, and $R_2(\omega_2,0,-\omega_1)$ are triply resonant when $\omega_2=\Omega(0,q)-\omega(0)$; the dephasing-induced terms $R_5(\omega_2,0,\omega_1)$ and $R_5(\omega_2,0,-\omega_1)$ are triply resonant when $\omega_2=\Omega(k,q)-\omega(k)$, and $R_1(\omega_2,\omega_2-\omega_1,\omega_2)$, $R_1(\omega_2,\omega_2-\omega_1,-\omega_1)$, and $R_1(\omega_2,0,\omega_1)$ are triply resonant when $\omega_2=\omega(0)$. In the superradiant limit, setting $\hat{\Gamma}=0$ eliminates the R_5 contribution; $R_2(\omega_2,0,\omega_1)$, $R_2(\omega_2,0,-\omega_1)$, and $R_3(\omega_2,\omega_2+\omega_1,\omega_1)$ are then responsible for a series of biexciton absorption lines, one for each value of q, with $q=1$ corresponding to the largest peak. In Fig. 6 we show the differential probe absorption spectrum (absorption spectrum in the presence of the pump minus the spectrum with no pump). This is given by $\mathrm{Im}\chi^{(3)}(-\omega_2,-\omega_1,\omega_2,\omega_1)$ and clearly reveals the $q=1$, 3, and 5 biexciton peaks lying to the red of the exciton peak for positive values of V. The exciton peak arises from the triple resonances in R_1. Notice that the exciton peak and the biexciton peaks carry opposite signs. The initial exciton population created by the pump beam serves to amplify the probe beam (via stimulated emission) when it is tuned to the exciton absorption peak, leading to a positive differential absorption. The initial exciton population also enables the probe to be absorbed more strongly when its frequency matches the exciton-biexciton transition $\Omega(0,q)-\omega(0)$. This leads to a negative differential absorption. Also notice that all biexciton line shapes

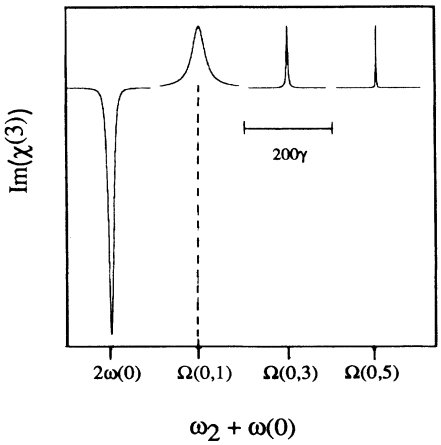

FIG. 6. Differential absorption spectrum, $\mathrm{Im}[\chi^{(3)}(-\omega_2;\omega_2,-\omega_1,\omega_1)]$ vs $\omega_2+\omega(0)$ for $N=21$. The pump-beam frequency ω_1 is equal to ω_0+2V and the probe-beam frequency is ω_2. The homogeneous dephasing rate $\hat{\Gamma}$ is zero. The negative peak is due to saturated exciton absorption, while the positive peaks are biexciton absorption spectra for $q=1$, 3, and 5 and $k=0$ as indicated. When $V>0$ these peaks lie to the red of the exciton peak.

have equal values at the absorption peaks but exhibit smaller linewidths for higher q values. This is a manifestation of the fact that biexcitons with higher q values have smaller superradiant damping rates $\Gamma(0,q)$, but also smaller weighting factors I_q which are reduced in the same proportion, i.e.,

$$I_q/\Gamma(0,q)=2[(N-1)\gamma]^{-1}, \tag{7.1}$$

which is obviously independent of q.

Figures 7(a) and 7(b) show the effects of pure dephasing on the exciton and biexciton absorption peaks, respectively. Note the appearance of the narrow resonance in the exciton peak. This arises from the time-ordered interaction with the pump beam followed by the probe beam and finally with the pump beam again. This process is triply resonant in $R_1(\omega_2,\omega_2-\omega_1,-\omega_1)$. Scanning the probe-beam frequency through $\omega(0)$ produces the narrow resonance which can be traced to the two-photon Green function.

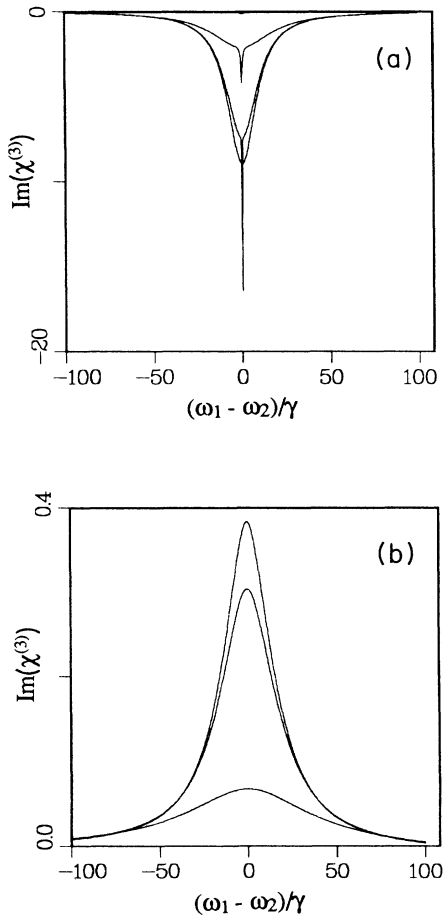

FIG. 7. Differential absorption spectra $\mathrm{Im}[\chi^{(3)}(-\omega_2;\omega_2,-\omega_1,\omega_1)]$ vs $\omega_1-\omega_2$ for $N=21$. (a) The $k=0$ exciton absorption line is shown for $\hat{\Gamma}/N\gamma=0$, 0.01, 0.1, and 1.0. (b) The $k=0$, $q=1$ biexciton spectrum is shown for the same values of $\hat{\Gamma}$. In both cases the peak magnitude decreases as $\hat{\Gamma}$ is increased.

VIII. CONCLUSION

We have calculated the nonlinear susceptibility $\chi^{(3)}$ of a distribution of small ($k_0 r_{mn} \ll 1$) molecular aggregates, allowing for homogeneous dephasing. Throughout the calculation interaggregate interactions have been neglected. This is justified only if the local electric field acting on a particular aggregate, which is composed of the applied field plus the field generated by all other aggregates, can be safely approximated by the applied field only. When inhomogeneous broadening is included this approximation is easier to justify. By the arguments of Ref. 13 the system must be (1) optically thin and (2) dilute, so that the number density η satisfies $\eta \ll \sigma/(N\gamma\lambda^3)$. Condition (1) ensures the neglect of macroscopic, interaggregate superradiance and condition (2) prevents energy transfer among neighboring aggregates.

The general expression for $\chi^{(3)}$ has a complicated N dependence which is a function of the particular nonlinear technique, the homogeneous dephasing $\hat{\Gamma}$ and the detuning of the laser beams. *An important conclusion to be drawn from this work is that $\chi^{(3)}$ does not show in general a universal enhancement with size, and that under off-resonant conditions it shows no enhancement at all.* For phase-conjugate degenerate four-wave mixing with $\hat{\Gamma} \ll N\gamma$, larger aggregates display smaller values of $\chi^{(3)}$ when the pump beams are tuned to the exciton absorption peak. The number of photons per second emitted in the phase-conjugate direction and integrated over $\omega_1-\omega_2$, $S(N,\hat{\Gamma},\Delta\omega_1)$, is inversely proportional to N. In the opposite limit ($\hat{\Gamma} \gg N\gamma$), $S(N,\hat{\Gamma},\Delta\omega_1)$ is enhanced over the monomer dependence by a factor of N^2. However, when the pump beams are off resonance there is *no enhancement* and the monomer result is recovered. We also predict a narrow dephasing-induced resonance in the phase-conjugate DFWM spectrum, which is an indirect measurement of the subradiant exciton states. For small dephasing values, the linewidth is $\hat{\Gamma}/N$ and the narrow line is superposed on a broad superradiant peak. The superradiant linewidth is linearly proportional to the aggregates size N and may thus be used to experimentally determine the aggregate size. As $\hat{\Gamma}$ increases to values much greater than $N\gamma$, the resonance linewidth converges to a width of γ. In this limit the aggregate exhibits its collective properties as well as independent molecular properties. The DFWM spectrum is a maximum when the pump beams are tuned to the exciton frequency ω_0+2V, but the radiative linewidth is characteristic of a single molecule.

Finally, we have calculated the biexciton absorption spectrum in the presence of a pump. It consists of a series of $(N-1)/2$ equal height absorption lines with steadily decreasing radiative linewidths given by Eq. (3.7b) as the index q increases. For sufficiently high q values the biexciton states become subradiant.

ACKNOWLEDGMENTS

We wish to thank D. Chemla for most useful discussions. We are pleased to thank the photographic research laboratories of the Eastman Kodak Company for their assistance in this work. The support of the National Science Foundation, the Office of Naval Research, and the Petroleum Research Fund, administered by the American Chemical Society, is gratefully acknowledged. S.M. has received support from the Camille and Henry Dreyfus Foundation.

APPENDIX A

In this appendix we show that the Liouville operator L_2 does not contribute to the diagonal matrix elements of $\mathcal{G}^0(\omega)=1/(\omega-L_1-L_2)$ [Eq. (4.9)]. We begin by showing that the off-diagonal matrix elements

$$\langle\langle n^{(i)}\overline{m^{(j)}}|\mathcal{G}^0(t)|n'^{(i')}\overline{m'^{(j')}}\rangle\rangle \quad (n,n,n',m'=0,1,\ldots,N) ,$$

are zero for all time when $n>n'$ and $m>m'$. Here, we use a more general notation to denote the eigenstates of L_1. The state $|n^{(i)}\rangle\rangle$ corresponds to $|n^{(i)}\rangle\langle 0|$, where $|n^{(i)}\rangle$ denotes the ith eigenstate in the nth-excited-state manifold. For example, $n=1$ for all N exciton states ($i=1,2,\ldots,N$) and $n=2$ for all $N(N-1)/2$ biexciton states [$i=1,2,\ldots,N(N-1)/2$].

To show why this matrix element is zero we begin by writing its equation of motion. Substituting $|\rho(t)\rangle\rangle=\mathcal{G}^0(t)|\rho(0)\rangle\rangle$ into Eq. (2.7) (neglecting $L_{\rm int}$) we obtain

$$\frac{d\mathcal{G}^0(t)}{dt}=-i(L_1+L_2)\mathcal{G}^0(t) , \tag{A1}$$

which for the element in question becomes

$$\frac{d\langle\langle n^{(i)}\overline{m^{(j)}}|\mathcal{G}^0(t)|n'^{(i')}\overline{m'^{(j')}}\rangle\rangle}{dt}=[i(\omega_n^i-\omega_m^j)-(\gamma_m^i+\gamma_n^i)]\langle\langle n^{(i)}\overline{m^{(j)}}|\mathcal{G}^0(t)|n'^{(i')}\overline{m'^{(j')}}\rangle\rangle$$
$$-i\sum_\beta\langle\langle n^{(i)}\overline{m^{(j)}}|L_2|\beta\rangle\rangle\langle\langle\beta|\mathcal{G}^0(t)|n'^{(i')}\overline{m'^{(j')}}\rangle\rangle , \tag{A2}$$

where $-\omega_n^i-i\gamma_n^i$ is the eigenvalue of L_1 corresponding to $|n^{(i)}\rangle\rangle$ and $|\beta\rangle\rangle$ is the complete eigenbasis of L_1. Since $-iL_2Q=N\gamma b_0 Q b_0^\dagger$, the only eigenvectors $|\beta\rangle\rangle$ which will lead to a nonzero term in the summation are $|\beta\rangle\rangle=|(n+1)^{(k)}(m+1)^{(l)}\rangle\rangle$. In order to solve Eq. (A2) we need to now how $\langle\langle(n+1)^{(k)}\overline{(m+1)^{(l)}}|\mathcal{G}^0(t)|n'^{(i')}\overline{m'^{(j')}}\rangle\rangle$ evolves in time. This would require solving another equation of motion similar to Eq. (A2) for this element, in which $\langle\langle(n+2)^{(r)}\overline{(m+2)^{(s)}}|\mathcal{G}^0(t)|n'^{(i')}\overline{m'^{(j')}}\rangle\rangle$ would appear as a source term on the right-hand side. This hierarchy will continue p times until either $n+p$ or $m+p$ becomes equal to N, at which point the equation of motion becomes (in the case of $n+p=N$, for example)

$$\frac{d\langle\langle N^{(s)}\overline{(m+p)^{(t)}}|\mathcal{G}^0(t)|n'^{(i')}\overline{m'^{(j')}}\rangle\rangle}{dt}=[i(\omega_N^s-\omega_{m+p}^t)-(\gamma_N^s+\gamma_{m+p}^t)]\langle\langle N^{(s)}\overline{(m+p)^{(t)}}|\mathcal{G}^0(t)|n'^{(i')}\overline{m'^{(j')}}\rangle\rangle . \tag{A3}$$

Now, the solution of Eq. (A3) is simply the initial condition times

$$\exp\{i[(\omega_N^s-\omega_{m+p}^t)-(\gamma_N^s+\gamma_{m+p}^t)]t\} ,$$

however, the initial condition for any off-diagonal Green-function matrix element is zero since

$$\mathcal{G}^0(t=0)=\mathbb{1} , \tag{A4}$$

where $\mathbb{1}$ is the identity matrix. It follows that the matrix element is zero for all times. The next set of equations in the hierarchy (with $n=N-1$) will now be missing source terms and because of Eq. (A4) they also will also be zero for all time. Continuing in this fashion one can show that all off-diagonal matrix elements (with $m>m'$ and $n>n'$) are zero for all time. (Physically this corresponds to the fact that there is no coupling mechanism which can transfer coherence or population from a lower-energy manifold to a higher-energy one.) It is now straightforward to show that the diagonal Green-function matrix elements are unaffected by L_2. Since $n=n'$ and $m=m'$ in a diagonal element, the equation of motion will contain a source term which contains an off-diagonal matrix element $\langle\langle(n+1)^{(k)}\overline{(m+1)^{(l)}}|\mathcal{G}^0(t)|n^{(i')}\overline{m^{(j')}}\rangle\rangle$. As we have just shown, this element is equal to zero, and therefore the diagonal matrix elements are independent of L_2.

APPENDIX B

In this appendix we calculate the off-diagonal Green-function matrix elements

$$\langle\langle 0|\mathcal{G}^0(t)|b(0)\bar{b}(0)\rangle\rangle$$

and

$$\langle\langle b(0)|\mathcal{G}^0(t)|B(0,q)\bar{b}(0)\rangle\rangle .$$

The first element describes the ground-state feeding from the $k=0$ exciton population due to superradiance and the second represents the superradiant decay of the three-body exciton-biexciton coherence to an exciton coherence. These elements are in a class of off-diagonal matrix elements represented by

$$\langle\langle n^{(i)}\overline{m^{(j)}}|\mathcal{G}^0(t)|n'^{(i')}\overline{m'^{(j')}}\rangle\rangle ,$$

(in the notation of Appendix A), with $n<n'$ and $m<m'$ and may therefore be nonzero. By the same arguments in Appendix A,

$$\langle\langle 0|\mathcal{G}^0(t)|b(0)\bar{b}(0)\rangle\rangle$$

can be shown to satisfy the equation of motion:

$$\frac{d\langle\langle 0|\mathcal{G}^0(t)|b(0)\bar{b}(0)\rangle\rangle}{dt}=-i\sum_{\beta}\langle\langle 0|L_1+L_2|\beta\rangle\rangle\langle\langle\beta|\mathcal{G}^0(t)|b(0)\bar{b}(0)\rangle\rangle , \tag{B1}$$

which further reduces to

$$\begin{aligned}\frac{d\langle\langle 0|\mathcal{G}^0(t)|b(0)\bar{b}(0)\rangle\rangle}{dt}&=-i\langle\langle 0|L_2|b(0)\bar{b}(0)\rangle\rangle\langle\langle b(0)\bar{b}(0)|\mathcal{G}^0(t)|b(0)\bar{b}(0)\rangle\rangle\\&=N\gamma\langle\langle b(0)\bar{b}(0)|\mathcal{G}^0(t)|b(0)\bar{b}(0)\rangle\rangle .\end{aligned} \tag{B2}$$

Substituting

$$\langle\langle b(0)\bar{b}(0)|\mathcal{G}^0(t)|b(0)\bar{b}(0)\rangle\rangle=\exp(-iN\gamma t)$$

[Fourier transform of Eq. (4.9b)] and taking the one-sided Fourier transform yields

$$\langle\langle 0|\mathcal{G}^0(\omega)|b(0)\bar{b}(0)\rangle\rangle=\frac{1}{\omega}-\frac{1}{\omega+iN\gamma} . \tag{B3}$$

In order to calculate

$$\langle\langle b(0)|\mathcal{G}^0(t)|B(0,q)\bar{b}(0)\rangle\rangle ,$$

we follow the same procedure. Its equation of motion is

$$\begin{aligned}\frac{d\langle\langle b(0)|\mathcal{G}^0(t)|B(0,q)\bar{b}(0)\rangle\rangle}{dt}&=i\left[\omega(0)+i\frac{N\gamma}{2}\right]\langle\langle b(0)|\mathcal{G}^0(t)|B(0,q)\bar{b}(0)\rangle\rangle\\&\quad+4\gamma\sum_{q\ \text{odd}}^{N-2}\cot\frac{\pi q}{2N}\langle\langle B(0,q)\bar{b}(0)|\mathcal{G}^0(t)|B(0,q)\bar{b}(0)\rangle\rangle ,\end{aligned} \tag{B4}$$

from which the formal solution can be written

$$\begin{aligned}\langle\langle b(0)|\mathcal{G}^0(t)|B(0,q)\bar{b}(0)\rangle\rangle&=\exp\left[\left[i\omega(0)-\frac{N\gamma}{2}\right]t\right]\\&\quad\times\int_0^t 4\gamma\sum_{q\ \text{odd}}^{N-2}\cot\frac{\pi q}{2N}\exp\{i[\Omega(0,q)-2\omega(0)]t'-[\Gamma(0,q)+N\gamma]t'\}dt' ,\end{aligned} \tag{B5}$$

where Eq. (A4) has been used. This reduces to

$$\begin{aligned}\langle\langle b(0)|\mathcal{G}^0(t)|B(0,q)\bar{b}(0)\rangle\rangle&=\sum_{q\ \text{odd}}^{N-2}\cot\frac{\pi q}{2N}\frac{4\gamma}{i[\Omega(0,q)-2\omega(0)]-[\Gamma(0,q)+N\gamma]}\\&\quad\times\exp\left[\left[i\omega(0)-\frac{N\gamma}{2}\right]t\right](\exp\{i[\Omega(0,q)-2\omega(0)]t-[\Gamma(0,q)+N\gamma]t\}-1)\end{aligned} \tag{B6}$$

The entire right-hand side is negligible and

$$\langle\langle b(0)|\mathcal{G}^0(t)|B(0,q)\bar{b}(0)\rangle\rangle$$

is approximately zero for all time when

$$\left|\frac{2N\gamma}{\pi V[\cos(\pi q/N)-1]}\right|\ll 1 , \tag{B7}$$

which is essentially the same as condition (3.8), which we have assumed from the start.

[1]B. Kopainsky and W. Kaiser, Chem. Phys. Lett. **88**, 357 (1982); B. Kopainsky, J. K. Hallermeier, and W. Kaiser, *ibid.* **83**, 498 (1981); P. O. J. Scherer and S. F. Fischer, Chem. Phys. **86**, 269 (1984).

[2]A. P. Alivisatos, M. F. Arndt, S. Efrima, D. H. Waldeck, and C. B. Harris, J. Chem. Phys. **86**, 6540 (1987); I. Kemnitz, N. Tamai, I. Yamazaki, N. Nakashima, and K. Yoshihara, J. Phys. Chem. **90**, 5094 (1986).

[3]M. Y. Hahn and R. L. Whetten, Phys. Rev. Lett. **61**, 1190 (1988); U. Even, N. Ben-Horin and J. Jortner, *ibid.* **62**, 140 (1989); S. Leutwyler and J. Bosiger, Chem. Rev. (to be published).

[4]G. Scheibe, Angew. Chem.. **50**, 212 (1937); E. E. Jelly, Nature (London) **10**, 631 (1937); A. H. Hertz, Adv. Colloid Interface Sci. **8**, 237 (1977).

[5]E. W. Knapp, Chem. Phys. **85**, 73 (1984).

[6]S. DeBoer, K. J. Vink, and D. A. Wiersma, Chem. Phys. Lett. **137**, 99 (1987); D. A. Wiersma and D. DeBoer, in *Ultrafast Phenemona VI,* edited by T. Yajima, K. Yoshihara, C. B. Harris, and S. Shionoya (Springer-Verlag, Berlin, 1988), p. 354.

[7]V. Sundstrom, T. Gillbro, R. A. Gadonas, and A. Piskarskas, J. Chem. Phys. **89**, 2754 (1988); H. Stiel, S. Daehne, and K. Teuchner, J. Lumin. **39**, 351 (1988).

[8]D. V. Brumbaugh, A. A. Muenter, W. Knox, G. Mourou, and B. Wittnerhaus, J. Lumin. **31**, 783 (1984).

[9]V. Mizrahi, G. I. Stegeman, and W. Knoll, Phys. Rev. A **39**, 3555 (1989).

[10]J. Grad, G. Hernandez, and S. Mukamel, Phys. Rev. A **37**, 3838 (1988).

[11]F. C. Spano and S. Mukamel, J. Chem. Phys. **91**, 683 (1989).

[12]M. Gross and S. Haroche, Phys. Rep. **93**, 301 (1982); R. H. Lehmberg, Phys. Rev. **2**, 883 (1970).

[13]*Optical Nonlinearities and Instabilities in Semiconductors,* edited by H. Haug (Academic, New York, 1988); A. Stahl and I. Balslev, *Electrodynamics of the Semiconductor Band Edge* (Springer-Verlag, Berlin, 1987).

[14]*Nonlinear Optical Properties of Organic Molecules and Crystals,* edited by D. S. Chemla and J. Zyss (Academic, New York, 1987), Vols. 1 and 2.

[15]D. S. Chemla, D. A. B. Miller, P. W. Smith, A. C. Gossard, and W. Wiegmann, IEEE J. Quantum Electron. **QE-20**, 265 (1984).

[16]L. Banyai, I. Galbraith, and H. Haug, Phys. Rev. B **38**, 3931 (1988); H. Haug and S. Schmitt-Rink, J. Opt. Soc. Am. B **2**, 1135 (1985).

[17]G. P. Agrawal and C. Flytzanis, Chem. Phys. Lett. **44**, 366 (1977); G. P. Agrawal, C. Cojan, and C. Flytzanis, Phys. Rev. B **17**, 776 (1978).

[18]J. W. Wu, J. P. Heflin, R. A. Norwood, K. Y. Wong, O. Zamani-Khamiri, A. F. Garito, P. Kalyanaraman, and J. Sounik, J. Opt. Soc. Am. B **6**, 707 (1989).

[19]Y. R. Kim, M. Lee, J. R. G. Thorne, R. M. Hochstrasser, and J. M. Ziegler, Chem. Phys. Lett. **145**, 75 (1988).

[20]L. Brus, IEEE J. Quantum Electron. **QE-22**, 1909 (1986).

[21]Y. Wang, A. Suna, W. Mahler, and R. Kasowski, J. Chem. Phys. **87**, 7315 (1987).

[22]S. Schmitt-Rink, D. A. B. Miller, and D. S. Chemla, Phys. Rev. B **35**, 8113 (1987).

[23]L. Banyai, M. Lindberg, and S. W. Koch, Opt. Lett. **13**, 212 (1988); L. Banyai, Y. Z. Hu, M. Lindberg, and S. W. Koch, Phys. Rev. B **38**, 8142 (1988); L. Banyai, I. Galbraith, and H. Haug, *ibid.* **38**, 3931 (1988).

[24]E. Hanamura, Phys. Rev. B **37**, 1273 (1988); **38**, 1228 (1988).

[25]H. Haken and G. Strobl, Z. Phys. **262**, 135 (1973).

[26]A. Yariv and P. Yeh, *Optical Waves in Crystals* (Wiley, New York, 1984); W. R. Tompkin, M. S. Malcuit, R. W. Boyd, and J. E. Sipe, J. Opt. Soc. Am. B **6**, 757 (1989).

[27]D. Pavolini, A. Crubellier, P. Pillet, L. Carbaret, and S. Liberman, Phys. Rev. Lett. **54**, 1917 (1985).

[28]J. T. Remillard, H. Wang, D. G. Steel, J. Oh J. Pamulapati, and P. K. Bhattacharya, Phys. Rev. Lett. **62**, 2861 (1989).

[29](a) S. E. Schwartz and T. Y. Tan, Appl. Phys. Lett. **10**, 4 (1967); (b) R. W. Boyd and S. Mukamel, Phys. Rev. A **29**, 1973 (1984).

[30]M. Veta, H. Kanzaki, R. Kobayoshi, Y. Toyozawa, and E. Hanamura, *Excitonic Processed in Solids* (Springer-Verlag, New York, 1986).

[31]H. Haug and S. Schmitt-Rink, Prog. Quantum. Electron. **10**, 1 (1984).

[32]I. Abrahm, Phys. Rev. B **28**, 4433 (1983); **29**, 4480 (1984).

[33]R. Levy, B. Honerlage, and J. B. Grun, in Ref. 14, Chap. 8.

[34]S. Mukamel and R. F. Loring, J. Opt. Soc. Am. B **3**, 595 (1986); S. Mukamel, Phys. Rep. **93**, 3 (1982).

[35]P. N. Butcher, *Nonlinear Optical Phenomena* (Ohio University Press, Athens, OH, 1965).

[36]Y. R. Shen, *The Principles of Nonlinear Optics* (Wiley, New York, 1984).

[37]R. F. Loring and S. Mukamel, J. Chem. Phys. **85**, 1950 (1986).

[38]E. N. Economou, *Green's Functions in Quantum Physics* (Springer, New York, 1983).